Unusual subduction zones: Case studies in Colombia and Iran

Zoya Zarifi

Thesis for the degree of Philosophiae Doctor (PhD)

at the University of Bergen

November 2006

Acknowledgements

I am grateful to a large number of people who have supported me during my Ph.D. on a professional as well as personal level.

First I would like to thank to my supervisors Kuvvet Atakan, Jens Havskov and Andrzej Hanyga for their supervision and support, for the valuable discussions and for providing a nice environment for their students. Thanks to all the staff at the Geodynamics group for their scientific support. I would like to especially thank to Eystein S. Husebye and Ritske S. Huismans.

I am grateful to the Norwegian State Loan Funds for providing the financial support for my Ph.D studies.

The present thesis summary benefited from comments and suggestions from my supervisors as well as from Anna Ksienzyk, Mohammad Raeesi and Aleksandre Kandilarov.

I would like to thank to Berit Marie Storheim, Annelise Kjærgaard and Norbjørg Kaland at Department of Earth Science for their continuous support. I wish to thank to all my colleagues, who have helped me throughout my work and have been good friends. Here I would like to mention Berit Marie Storheim, Anita Torabi, Nada Bushra-Eltahir, Claudia Kruber, Karleen Black, Mathilde Bøttger Sørensen, Louise Bjerrum, Anna Ksienzyk, Alexandre Kandilarov and Hlompo Malephane.

At last but certainly not least, I wish to thank to my family. Thanks to my husband, Mohammad Raeesi, for being my best friend and always supportive. Thanks to my dear son, Arya Raeesi, who has been a good kid and although just 3 years old, he could understand that Mammy needed to work hard. I am grateful to my mother, Gohar Ghomshe, for all she has done for me. I thank my sister Faranak and my brothers Keyvan and Siyamak for being a great inspiration for me. Thanks to my other family members, Baharak Saraffan, Sima and Keyvaneh Raeesi for their support.

Preface

The work presented in this thesis was initiated in August 2001, when I was enrolled in the Ph.D. program of the University of Bergen (UIB). According to the regulations of UIB, the first part of this thesis is a “summary” of the work I have done during my Ph.D. studies and the future challenges within the described topics. This part is meant to provide the overview of the entire research conducted and the relations between the papers. In this sense there is inevitably repetitions between part I and II, however there is also additional information and discussion on the individual results that are presented in the papers in part II. The second part, which is the main outcome of my studies, is a collection of four research papers, which are all currently either published or are in revision and review for publication in international journals.

The focus of this thesis is the unusual seismic behavior in the subduction zones, with two case studies in Colombia and Iran. The first part of this thesis, includes 6 sections. The first section briefly explain the objective of the thesis and the challenges that we faced and strategies that we made to overcome the problems. The second section explain the unusual high rate of dense seismic activity in the subduction zone throughout the world and focuses in one the most disputable one in Colombia. More details of our investigations in this topic are addressed in the first and second papers. The third section explain the unusual low rate or lack of seismic activity at the slab interface of the Makran subduction zone in the southeast of Iran and southern Pakistan. The details of our investigation in Makran are addressed in the third and fourth papers. The fourth section discusses our observation and the fifth section is the summary of our achievements. The sixth section is an outlook of what needs to be done in the future.

In the second part of the thesis, I estimate my contribution to the papers to be as follows:

The first paper, “Characteristics of dense nests of deep and intermediate depth seismicity”, which has been published in 2003, in Advances in Geophysics, 85%.

The second paper, “An insight into the Bucaramanga nest”, which is in revision in Tectonophysics, 90%.

The third paper, “The Makran subduction zone (Part I): Current state of crustal stress”, which is in review in BSSA, 85%.

The fourth paper, “The Makran subduction zone (Part II): Seismogenic behavior in the fore-arc setting”, which is in review in BSSA, 90%.

Zoya Zarifi,

November 2006

Abstract

Subduction zones, usually, are plate boundaries with the highest level of seismic activity. However, the distribution of seismicity in these plate margins is not uniform in the frequency and magnitude. Some margins produce frequent earthquakes of only moderate size, some experience great earthquakes separated by periods of little to moderate size activity, while others may have no plate boundary earthquakes during historical time. In the latter it is difficult to ascertain if the subduction zone is strongly coupled or the slab is subducting aseismically. In addition, the distribution of the seismic activity at intermediate depths does not follow a uniform pattern. The abundance of intermediate depth earthquakes show a marked onset at a depth of 30-70 km and then decrease exponentially with increasing depth. However, there are areas at intermediate depths (mostly, deeper than 100 km) that experience a very high rate of stationary seismic activity, the so called “earthquake nests”. The aim of this research is to address the unusual seismicity observed in subduction zones with focus in mainly two areas. First part of the thesis deals with the Bucaramanga nest in Colombia, where Nazca and Caribbean plates converge towards the south American plate and subducting beneath the north Andes block. This area has been marked with complexity in the tectonic settings, lack of volcanoes and high rate of dense seismic activity at intermediate depths. The second part focuses in the Makran subduction zone, in south east of Iran and southern Pakistan, where the oceanic crust of the Oman sea is subducting beneath the Eurasian plate. In this area, the slab interface has been marked with low rate of seismic activity.

In order to have an overview of the characteristics and the physical reason behind the nature of the Bucaramanga nest, we first investigated all reported and possible earthquake nests in the world. A general investigation in geometrical, seismological and tectonical aspects of earthquakes nests in Romania (Vrancea), Afghanistan (Hindu Kush), Colombia (Bucaramanga) and a few reported possible nests in Fiji, Ecuador and Chile-

Argentina border reveal that among all these nests, the smallest and the most active is the Bucaramanga nest. On the other hand, the nature of the Bucaramanga nest is the most disputable compared to the other earthquake nests. We studied the local seismicity obtained from National Network of Colombia from 1993-2001 in and around the Bucaramanga nest. The local data reveals two slabs subducted in the north and south of the Bucaramanga nest. The dip angles of the slabs in the north and south of the Bucaramanga nest are different (about $25°$in the north and $50°$in the south). The dip angle of the Bucaramanga nest is about $29°$, in a good agreement with the northern slab. However, the result we obtained from focal mechanism stress inversion of moderate size earthquakes in the nest, shows that Bucaramanga is experiencing down dip extension, where the plunge of σ_3 is more in agreement with the dip angle southern slab. The fault mechanisms of earthquakes in the Bucaramanga nest show considerable non-double couple components which reveal source complexity in the nest. Also some variation in the mechanism of earthquakes in the nest can be observed based on Harvard catalog. Using a 3D Finite Element Modelling (FEM), with elastic lithosphere and inviscid fluid mantle, we show how collision between the two slabs could concentrate and modify the stress field. The concentrated stress field can explain the high rate of seismic activity in the area of the nest and the modified stress field can answer the variation in the observed focal mechanisms and the source complexity of the earthquakes in the Bucaramanga nest. We therefore suggest that the collision between the subducting slabs is the cause of the Bucaramanga nest.

In the second part of thesis, we studied the Makran subduction zone to address the reason for the low rate of seismic activity at the slab interface. In Makran, the oceanic crust of the Oman sea subducts with a very low angle beneath the Eurasian plate. It is bounded to the west by continent- continent collision between Arabia and Eurasia and to the east by continent- continent collision between Indian and Eurasian plates. This subduction zone exhibits different seismic behavior in its fore-arc setting from the west toward the east. The entire eastern Makran has been ruptured throughout history by large earthquakes and currently is experiencing very low seismic activity in its fore-arc setting. However, the western Makran looks quiet and there is only one known earthquake in historical time, which could have occur in this region. The overriding lithosphere in Makran is marked with segmentation along the Sistan suture zone. The seismicity in Makran shows a steeper slab in the west compared to the east. The absence of seismicity in the fore-arc setting of the western Makran prevents any estimate about the dip angle of slab where it starts bending beneath the overriding lithosphere. However, we used the free air gravity anomaly in the trench area of the western and the eastern Makran to show that the western Makran is experiencing more negative anomaly than the eastern Makran. This indicates steeper dip angle in the western Makran compared to the eastern Makran, where slab bends below the overriding lithosphere.

We have also investigated the present state of crustal stress in the overriding lithosphere in Makran by using focal mechanism stress inversion. We expanded the area of investigation to the collision zone between Arabia and Eurasia along Zagros to the west and to the collision zone between Indian and Eurasian plates to the east in order to find out any possible influence of the stress field of the collision zones into the Makran stress field. The results show a clear rotation in the direction of the compressional stress axis from the west toward the east of Makran, where the western Makran is under the influence of Arabian-Eurasian collision zone and the eastern Makran is under the influence of Indian- Eurasian collision zone. Furthermore, to investigate any possible interaction between the Sistan suture zone and the low angle slab, we studied the source of three recent intermediate depth earthquakes at 80, 72 and 58 km depth around the Sistan suture using body wave inversion. The results show no source complexity for the earthquakes at 80 and 72 km depth, but a complex source for the earthquake at 58 km depth. This may indicate that Sistan suture has a thick root and meets the slab around 58 km depth.

In order to address the absence of seismic activity in the fore-arc setting of the western

Makran, we used the free air gravity anomaly and removed the effect of gravity anomaly perpendicular to the trench. The residual gravity anomaly now is under the influence of shallower structures. We produced Trench Parallel Gravity and Topography Anomaly (TPGA and TPTA, respectively) maps. The TPGA and TPTA maps show that the whole western Makran fore-arc setting is marked with TPGA < -50 mGal and TPTA< -750 m. Based on other studies, the areas in the fore-arc setting with the TPGA< -40 mGal and TPTA < -750 m are prone to the strongest earthquakes. The high coefficient of friction (i.e. strong coupling) in the slab interface can explain this phenomena. The western Makran is separated from the eastern Makran, by a small area of strongly positive TPGA and TPTA. The TPGA and TPTA in the eastern Makran are different from the west, which may confirm heterogeneous frictional properties along the fore-arc setting. We used a 2D elastic-viscoelastic Finite Element (FE) model to show how a high coefficient of friction in the contact zone controls the shear stress build up in the interplate interface. We assigned high coefficient of friction to the area with the most negative TPGA (<-50 mGal) and TPTA (-750 m) in the western Makran. The result shows that it takes several hundreds of years until the shear stress reaches the yield point. This may explain why western Makran is not experiencing seismicity at the present time.

Observation of intermediate depth earthquakes with normal mechanism indicates that the eastern Makran is in the mature stages of an earthquake cycle. We used a 2D elastic-viscoelastic FE model to study deformation in the overriding plate within a single cycle of earthquake, where the slab interface coupled heterogeneously. We used the rupture zone of the strongest earthquake in the eastern Makran in our model as the area of the strongest coupling in the slab interface. The result shows that the deformation is more pronounced in the overriding lithosphere above the strongly coupled segment. Considering different length for the cycle of earthquakes, we conclude that the shorter the cycle of earthquakes the faster is the rate of deformations, so the rate of deformation in the eastern Makaran should be faster than the western Makran. Since most of the interplate interface in Makran is onshore, the area of the stronger coupling can be located by continuous geodetic observations in the future.

List of publications

- Z. Zarifi, J. Havskov, 2003, Characteristics of dense nests of deep and intermediate depth seismicity, Advances in Geophysics, 46, 237-278.
- Z. Zarifi, J. Havskov, A. Hanyga, 2006, An insight into the Bucaramanga nest, in revision, Tectonophysics.
- Z. Zarifi, K.Atakan, 2006, The Makran subduction zone (Part I): Current state of crustal stress, in review, BSSA.
- Z. Zarifi, K. Atakan and A. Hanyga, 2006, The Makran subduction zone (Part II): Seismogenic behavior in the fore-arc setting, in review BSSA.

Contents

Part I.

Summary

1. Summary

1.1. Introduction

As the Oceanic lithosphere moves away from an oceanic ridge, it cools, thickens and becomes more dense because of thermal contraction. Although the basaltic rocks of the oceanic crust are lighter than the underlying mantle rocks, the colder subcrustal rocks in the lithosphere become sufficiently dense to make old oceanic lithosphere heavy enough to be gravitationally unstable with respect to the hot mantle rocks immediately underlying the lithosphere. Along the subduction zones where two plates converge, due to gravitational instability the oceanic lithosphere sinks in the Mantle (Turcotte & Schubert, 2002). Japan, Izu-Bonin-Mariana, Philippine, South America, Cascadia, Aleutian, Kuril-Kamchatka, New Brtitian-Solomon, New Hebrides, Tonga-Kermadec-New Zealand, Lesser Antilles, Aegean, Indonesia and Makran are all convergent margins marked by subduction zones. The subduction of the oceanic lithosphere gives rise to two different types of orogenic belts depending upon the nature of the overriding lithosphere (Dewey & Bird, 1970). Subduction beneath the oceanic lithosphere results in formation of an island arc and its associated tectonic features, while subduction beneath continental lithosphere gives rise to a linear mountain belt on the overriding plate margins, which runs parallel to the subduction zone. The subduction zones have been studied extensively for a number of reasons: first, the corresponding plate interfaces are responsible for some of the largest earthquakes ever recorded (Becker, 2002). Second, subduction process is thought to be related to the tectonic processes in the overriding plates, like formation of orogens in compressive regimes, volcanism and back arc spreading in extensional regimes (Becker, 2002). Third, because slab pull is a large (Forsyth & Uyeda, 1975) or the largest (Lithgow-Bertelloni & Richards, 1995) contribution to the forces that driving the tectonic plates.

In the present thesis, our main motivation is to understand the deformation processes

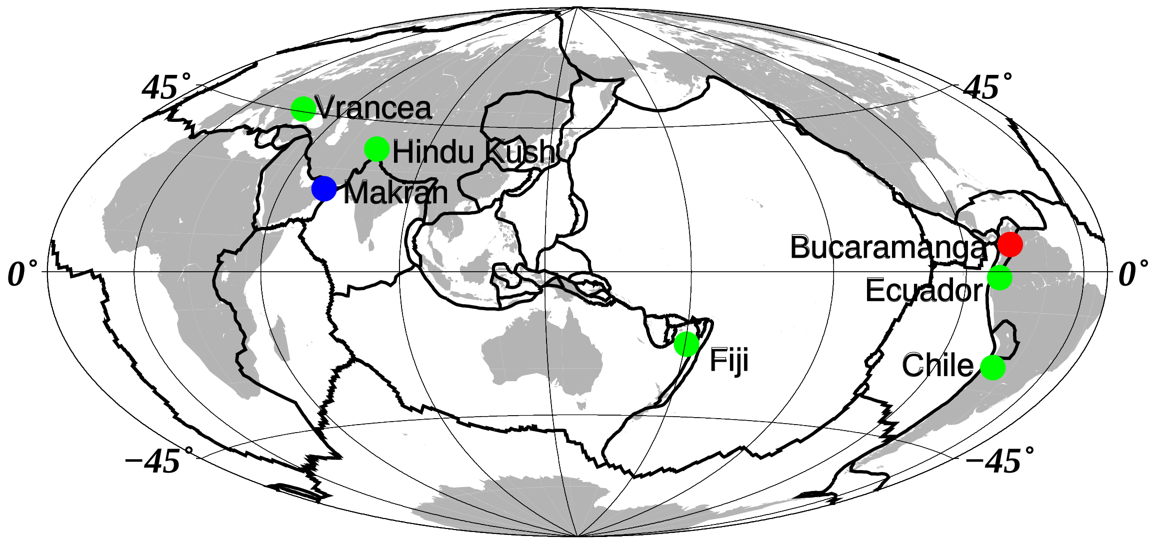

Figure 1: Areas of high and low level of seismic activity investigated in this research. The red circle, corresponds to the location of the Bucaramanga nest in Colombia, and the blue circle corresponds to the Makran subduction zone in the southeast of Iran and southern Pakistan. The green circles are the locations of the earthquake nests which have been reviewed.

along the subduction zones as expressed by the anomalous seismic activity.

Seismicity in subduction zones occurs as a result of four distinct processes: first, in the outer rise, the earthquakes occur in a response to the bending of the lithosphere as it begins its descent. Second, the contact area between the overriding and the underthrusting plates (shallower than 40 km), where the earthquakes occur due to compressional deformation. The slab interface is usually prone to the largest earthquakes ever recorded. Third at depths between 70-300 km, where it appears that faulting occurs during the rapid dehydration of Serpentinite or Amphibolite and fourth at depths below 300 km, where earthquakes mechanism is believed to be the sudden phase change from olivine to spinel, known as anticrack faulting (Kearey & Vine, 1996). It appears that high rate of seismic activity in shallower depths of subduction zone (at the outer rise and slab interface) decreases exponentially with increasing depth (at the intermediate and deep depths) (Frohlich *et al.*, 1989; Kirby *et al.*, 1996). However, it has been observed that the frequency and magnitude of seismicity is not always following the general rule mentioned above. There are areas at intermediate depths, in both style of subduction zones, which are marked with highly concentrated and continuous seismic activity (the so called 'earthquake nest'). Among them, Central America (Carr & Stoiber, 1973), New Zealand (Blot, 1981*a*), New Hebrides (Blot, 1981*b*), Aleutians (Engdahl, 1977), Colombia (Schneider *et al.*, 1987; Shih *et al.*, 1991*b*), Romania (Oncescu, 1984, 1986; Sperner *et al.*, 2001), Hindu Kush (Chatelain *et al.*, 1980; Burtman & Molnar, 1993) are well known for their unusual high rate of seismicity. The seismicity in earthquake nests are related to the melting in the upper surface of the underthrusted slab close to the active volcanoes (e.g. many places around Pacific and Indonesian arcs)(Carr, 1983) or to the complexity in the tectonic setting and processes like slab break off or collision between subducted slabs (e.g. the cases in Vrancea nest in Romania and also Hindu Kush nest in Afghanistan) (Sperner *et al.*, 2001; Santo, 1969). The latter, usually takes place where the oceanic lithosphere subducts beneath an continental lithosphere. Among all these earthquake nests at intermediate depths, the nature of the Bucaramanga nest in Colombia is more disputed. Different researches dealt with the nature of this nest and associated it with melt migration (Schneider *et al.*, 1987; Shih *et al.*, 1991*b*), concentration of stress field (Van der Hilst & Mann, 1994) or tearing of slab (Cortes & Angelier, 2005). Although, all proposed mechanisms partially explain some characteristics of the nest but still some questions cannot be answered. These are related to non existence of volcanic activity in and around the Bucaramanga nest, variation in the mechanism of earthquakes and complexity in the source of earthquakes. As part of this research, we study all earthquake nests related to complexity in the tectonic setting and then concentrate on the Bucaramanga nest to find a proper explanation to the observed characteristics of the nest. In order to investigate the Bucramanga nest, we studied the local seismicity and mechanism of earthquakes and proposed an explanation to the nature of this nest.

Further, using a 3D FE model, we demonstrate that the proposed process is feasible. Papers 1 and 2 in this research focus in this topic.

The unusual pattern of seismicity is not just associated with intermediate depths. There are also subduction zones which have not experienced large earthquakes in their slab interface in the modern time, like Cascadia and Lesser Antilles (Atwater, 1995; Fluck *et al.*, 1997; Adams, 1990; Stein *et al.*, 1982). In some others, like the western Makran, subduction zone marks an area with almost lack of seismic activity (Byrne *et al.*, 1992; Carayannis, 2006) in the slab interface. According to Pacheco *et al.* (1993), any unit of area along the plate interface is in one of the three possible state of frictional behavior: (1) stable, where the region slip stably without accumulating strain, (2) conditionally stable, where the region slips stably during the inter-seismic period between large earthquakes and (3) unstable, in region which are taken to be fully coupled. In the case of the above mentioned subduction zones, it is hard to ascertain that the slab interface is associated with which state of frictional behavior, stable or unstable. Numerous studies have associated Cascadia with unstable state of frictional behavior (Adams, 1990; Atwater, 1995; Satake *et al.*, 1996; Hyndman & Wang, 1995) and there are suggestion about stable state of frictional behavior in the Lesser Antilles subduction (Stein *et al.*, 1982). In the western Makran, however, there is no clear explanation about the lack of seismic activity (Farhoudi & Karig, 1977; Byrne *et al.*, 1992; Carayannis, 2006). The Makran subduction is a zone of convergence where the remnants of Neo-Tethys oceanic lithosphere is subducting beneath the continental lithosphere of Eurasian plate (Byrne *et al.*, 1992). In an attempt to explain the lack of seismic activity in the western Makran, we investigated the tectonic and seismogenic behavior of Makran subduction zone. In this research we address the state of stress, the gravitational anomaly in the fore-arc of Makran, a rough estimate of rate of shear stress build up in the western Makran and the deformation associated with the cycle of earthquakes in the eastern Makran. In papers 3 and 4, we use inversion methods and FE modelling to address and explain the problem.

All areas of investigation in this thesis are shown in Figure 1.

2. Unusual subduction zones- high rate of concentrated seismic activity at intermediate depths

For the details of this section, please refer to paper 1

2.1. Earthquake nests

A nest is defined by stationary seismic activity concentrated in a small volume, so that the seismic activity in this volume is substantially larger than in the surrounding areas. A seismic nest, with its continuous mode of seismic activity is different from swarm activity which take place occasionally. Within this definition two classes of nests can be defined. (A) intermediate or deep nests related to tectonic processes (e.g. slab break off and collision) in subduction zones and (B) shallow or intermediate depth nests related to volcanic activity in the overriding lithosphere and melt generation and migration in the mantle wedge. For the latter, there are numerous reports from the different parts of the world close to active volcanoes. Japan, Central America, New Zealand, New Hebrides and Aleutians are all marked with this kind of seismic activity (Usami & Watanabe, 1980; Carr & Stoiber, 1973; Blot, 1981*a*,*b*). However, the class (A) earthquake nests, don't have an unique explanation for their nature. The aim of the first paper is to give an overview of nests in class (A) which are related to tectonic processes and usually show no volcanic activity in their surroundings. Within this framework there are three well recognized nests, the Bucaramanga in Colombia, the Vrancea in Romania and the Hindukush in Afghanistan (Tryggvason & Lawson, 1970; Dewey, 1972; Schneider *et al.*, 1987; Frohlich *et al.*, 1995; Oncescu, 1984, 1986, 1987; Sperner *et al.*, 2001; Ojeda & Havskov, 2001). A few more have been suggested in Chile-Argentina border, Ecuador, Fiji, Italy and Burma (Tryggvason & Lawson, 1970; Schneider *et al.*, 1987). Figure 2 shows the location of recognized nests discussed in our first paper. In the next sections, the general feature of these nests will be explained briefly.

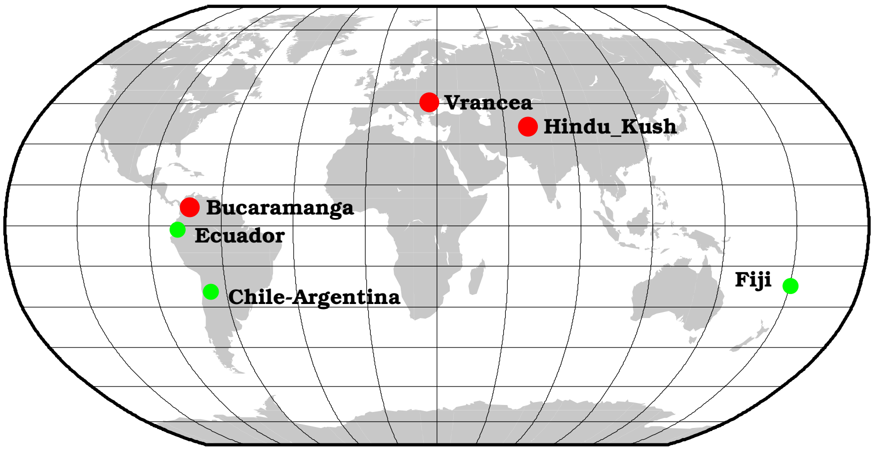

Figure 2: Location of known (red circles) and possible (green circles) nests in the world. The Bucaramanga nest is located in Colombia, the Hindu Kush in Afghanistan and the Vrancea in Romania.

2.2. Known nests

We used the ISC (1964-2000) and Harvard (1976-2003) catalogs in order to compare the common characteristics of the known nests in Colombia (Bucaramanga), Romania (Vrancea) and Afghanistan (Hindu Kush). Further, we review other studies to have a better understanding about the nature of these nests and to use our knowledge as a guide to recognize the other possible earthquake nests in the world. In the following sections, we address and compare the characteristics of each of the known nests.

2.2.1. Bucaramanga nest

The Bucaramanga nest, which is located in the north east of Colombia, is an intermediate depth nest centered around 160 km depth at about $6.8°N$ and $73.1°W$ (Tryggvason & Lawson, 1970; Schneider *et al.*, 1987; Dewey, 1972; Frohlich *et al.*, 1995; Ojeda & Havskov, 2001). The seismological characteristics of this nest are shown in Table 1. The majority of earthquakes inside the Bucaramanga nest have thrust mechanism (Based on Harvard CMT catalog), however variation in the mechanism of earthquakes in the nest is also considerable. The tectonic framework of Colombia is very complex. Many authors have discussed it but no clear conclusions have been reached (Taboada *et al.*, 2000; Kellogg & Vega, 1995; Malave & Suarez, 1995; Van der Hilst & Mann, 1994). Based on one of the latest tectonic models for Colombia made using local seismology, tectonics and global tomography, Taboada *et al.* (2000) have mentioned that, there are four plates which converge in this region: The North Andes block as part of the South American plate, the Panama block, the Caribbean and the Nazca plates. The tomographic image obtained by Van der Hilst & Mann (1994) suggests that there are two slabs in the eastern Colombia and the western Venezuela. The northern slab dips in a direction of 150° at an angle of 17° extends to a depth of 275 km and correlates with the subducted late Cretaceous oceanic plateau of the Caribbean plate. Further south, a second slab dips at an angle of 50° in a direction of 125° continues to a depth of at least 500 km and correlates with the subducted oceanic crust of the Nazca plate. There is no clear explanation about the physical reason behind the existence of the Bucaramanga nest. The most favored explanation, mainly based on variable observed focal mechanism of earthquakes in the Bucaramanga nest, is related to the generation and migration of fluids or to dehydration reactions. This means that the region is weakened by active fluid migration and mobilized by the heating and shearing along the subducting lithosphere (Schneider *et al.*, 1987; Shih *et al.*, 1991*a*). On the other hand, the existence of a complex stress field near the contact of the two subducted slabs could possibly explain such a dense seismic activity (Van der Hilst & Mann, 1994).

2.2.2. Vrancea nest

The Vrancea region in Romania is situated in a complex tectonic zone, which is characterized by clustered intermediate depth seismic activity (Oncescu, 1987). The Vrancea nest is located at 45.7°N and 26.5°E. The seismological characteristics of Vrancea are explained in Table 1. The mechanism of earthquakes (Based on Harvard catalog) in the Vrancea nest all show thrust faulting. The Vrancea seismic region is a complex tectonic zone, where the driving mechanism of intermediate depth events has been understood as

Table 1: Summary of the observed seismicity in the known nests. V is volume of the nest and V_N is the normalized volume, where $V_N = \frac{V}{V_{Hindu\,Kush}}$.

Nests	Bucaramanga	Vrancea	Hindu Kush
Location	6.8°N,73.1°W	45.7°N,26.5°E	36.5°N,71°E
Depth (km)	150-170	70-180	170-280
Size(ISC) (km^3)	33×35×35	25×55×110	60×80×100
Size(local) (km^3)	8×4×4	20×50×110	55×30×120
Normalized volume (ISC)(V_N)	0.084	0.32	1
Total number of events	2708	249	7096
Events M_b> 4.8	462	57	956
Number of events with M_b> 4.8 per (V_N)	5500	178	956
Average number of events with M_b> 4.8 per / month	1.1	0.13	2.2
b value	1.17	1.0	1.43
Largest reported event M_b in nest	6.4	6.4	6.5
Largest reported event M_b in surrounding area	5.7	5.0	6.0
Seismic moment release rate inside the nest (Nm/Y)	1.27E+23	1.48E+24	4.13E+24
Seismic moment release rate around the nest (Nm/Y)	2.44E+22	1.66E+21	6.82E+22

collision between three tectonic units, the Eastern-European platform, the Moesian sub-plate and the Inter-Alpine sub-plate (Oncescu, 1987). Bleahu *et al.* (1973) and Oncescu (1984) suggested that there is a NE-SW oriented paleo-subduction that is now decoupled from the crust and generating intermediate depth seismic activity of the Vrancea nest at the limit of the separation.

2.2.3. Hindu Kush nest

The Hindu Kush nest in Afghanistan is one of the most intriguing seismic zones of the world, because a large number of earthquakes occur in a limited zone (Nowroosi, 1972). The majority of these events are centered at 36.5°N, 71°E, within 175-250 km depth. The seismological characteristics of Hindu Kush are explained in Table 1. Based on Harvard catalog the mechanism of earthquakes inside the nest is thrust faulting. There are different views about the Hindu Kush tectonics. Some researchers suggested that the configuration of the Hindu Kush seismic nest defines a contorted Wadati-Benioff zone that dips to the north in the western end under Hindu Kush but dips southward at the eastern end of the zone under Pamir (Lukk & Nersesov, 1965; Lukk & Vinnik, 1975; Billington *et al.*, 1977). The opposing dips and a increase of seismicity where the two segments meet, imply that the zone consists of two distinct slabs with opposing directions of subduction (Fan *et al.*, 1994), but the possibility of a single contorted slab cannot be ruled out (Billington *et al.*, 1977). It seems that collision between two slabs from opposite direction or a contorted slab have concentrated the stress field and produce this high level of seismic activity.

2.3. Possible nests

There are some suggestions about other possible nests around the world. For example, Tryggvason & Lawson (1970) indicated that some dense source of intermediate and deep events in Burma and Italy might be earthquake nests. Also, Schneider *et al.* (1987) suggested that some clusters of events in Fiji, Ecuador and at the Chile-Argentina border may indicate earthquake nests. In the following sections, we used the common criteria for the three well-known nests to evaluate if the suggested seismicity can be considered nests like Bucaramanga, Vrancea and Hindu Kush. There are few published research paper about these nests and the comparison will therefore be based on global data. This cannot be conclusive since some nests may not be visible using global data. In fact, the recorded earthquakes in the ISC catalog failed to show any concentrated seismic activity in Burma and Italy, so we concentrate our research on those nests that can be addressed using global seismicity.

2.3.1. Fiji nest

There is a suggestion that the deep earthquakes in Fiji occur as multiple events, i.e. small numbers of events closely grouped in space and time (Isacks *et al.*, 1967). Among the reported location of multiples, at $22.2°S$ and $179.5°W$, we found concentrated seismic activity in the depth interval of 570-620 km, which may indicate an earthquake nest. Table 2 explains the characteristics of the Fiji nest. The dominant mechanism of earthquake in the nest is thrust faulting, which is strange for deep earthquakes (Richardson & Jordan, 2002). There is no explanation for such a high rate of seismic release in a small volume in Fiji, but according to Isacks *et al.* (1967), this possible nest is located in an area where there is some distortion in the depth distribution of deep earthquakes.

2.3.2. Ecuador nest

There is a report about the existence of a probable nest in Ecuador, which cannot be clearly detected with global data (Schneider *et al.*, 1987). By using ISC data, we found a weak concentration of seismic activity at $1.5°S$ and $78°W$, at depth interval of 150-200 km. The characteristics of this nest are shown in Table 2. The mechanism of earthquakes inside this possible nest is normal faulting. The existence of Cotopaxi volcano in Ecuador (at $0° 40^{'} S$ and $78° 26^{'} W$) may suggest that the nature of Ecuador nest can be different from the other nests addressed in our research, though this is uncertain.

2.3.3. Nest at Chile-Argentina border

Sacks *et al.* (1966) and Schneider *et al.* (1987) have reported an intermediate depth nest at the Chile-Argentina border in Socompa area, which has a famous volcano with the same name. Although this nest may be related to volcanic activity, but this is uncertain, and therefore we try to investigate the properties of this nest with the same criteria that we used to study the other nests. We found, that the Chile-Argentina nest is located at $24°S$ and $67.5°W$ in the depth interval between 168 and 220 Km. Table 2 explains the characteristics of the possible nest in Chile-Argentina border. The Harvard catalog shows normal faults as the dominant mechanism inside the possible nest at the Chile-Argentina border. Like Ecuador nest, the mechanism of earthquake here is different from the other nests in our research.

2.4. Earthquake nests - Overview

Regardless of the geographical location; the Bucaramanga, the Vrancea, the Hindukush and even the Fiji nests, are all located in complex tectonic settings in subduction zones. The b-value in these nests suggests normal tectonic activity (i.e. no swarm activity). The largest reported earthquakes in all these nests have almost the same magnitude (Mb=6.1-6.5), suggesting almost the same strength in the nest volume. The magnitude of the largest earthquakes in the surrounding area is less than the magnitude of the largest earthquakes inside the nest. The seismic moment release in the nests is higher than surroundings. The dominant mechanism of earthquakes in most of these nests is thrust faulting, however, the variation in the mechanism of earthquakes in the Bucaramanga nest is considerable. The mechanism of earthquakes in the Ecuador nest and the Chile-Argentina nest have no correlation with the rest of earthquake nests addressed in this research. Comparing the known nests based on ISC data reveals that the Hindu

Table 2: Summary of observed Seismicity in the possible nests. V is Volume of the nest and V_N is the normalized volume.

Nest	Fiji	Chile-Argentina	Ecuador
Location	22.2°S, 179.5°W	24°S, 67.5°W	1.5°S, 78°W
Depth (km)	570-620	168-220	150-200
Size (ISC)(km^3)	90×50×50	80×60×100	70×50×50
Normalized Volume ($V/V_{Hindu\,Kush}$)	0.47	1.0	0.36
Total number of events	277	776	173
Events with M_b>4.8	156	102	28
Number of events with M_b>4.8 per V_N	332	102	77
Average number of events with M_b>4.8 /month	0.36	0.23	0.06
b value	1.73	1.35	1.14
Largest reported event (M_b)	6.1	6.1	5.9
Largest reported event (M_b) in the surrounding area	5.5	5.1	5.5
Seismic moment release rate inside the nest (Nm/Y)	2.22E+23	1.55E+23	1.19E+23
Seismic moment release rate around the nest (Nm/Y)	5.22E+22	1.71E+23	8.10E+21

Kush nest has the largest volume comparing to the Bucaramanga and Vrancea nest. In fact, the volume of Hindu kush is about 12 times more than Bucaramanga and 3 times more than the Vrancea nest. We normalized the size of each nests to the size of Hindu Kush nest. Then by looking at the seismicity per normalized volume, we realised that the rate of seismic activity in Bucaramanga is about 6 times higher than in the Hindu Kush and about 30 times higher than in the Vrancea nest. The Bucaramanga seismicity is also significantly more than the seismicity in the possible nests. The physical reason behind the nature of the nests is well explained in the Vrancea nest and has been related to the process of slab break off. In Hindu Kush, collision between two slabs from opposite directions can be a possible explanation for concentration of the stress field and release of high rate seismic activity, while the physical reason behind the existence of the Bucaramanga nest has been explained as generation and migration of fluids or a concentrated stress field in the area of the nest. The nature of the possible nest is less studied and rather uncertain. In general, we conclude that the Bucaramanga nest is the smallest and the most active nest compared to the others, and also attracts more debate about its physical nature. Therefore, we further concentrate on the Bucaramanga nest, which is investigated in detail in the second paper.

2.5. Insight into the Bucaramanga nest

For the details of this study please refer to paper2

In the second paper, we investigated the Bucaramanga nest using local seimicity from the National Network of Colombia and reviewed all proposed mechanisms behind the nature of the Bucaramanga nest. We analyzed the mechanisms of earthquakes and the state of stress in the nest and furthermore proposed a different mechanism which may explain the nature of the nest. Figure 3 shows that Colombia exhibits a complex deformation with convergence of four plates: The north Andes block as part of the south American plate, the Panama block, the Caribbean and the Nazca plates. The northeast of Andes block is marked with high level of seismic activity in the Bucaramanga nest and lack of active volcanoes. We use this seismicity in the next section to view the 3D sections of the subducted slab in this region.

2.6. Local seismicity in Colombia and the Bucaramanga nest

We used all local data in the period of 1993-2001 reported by the National Seismic Network of Colombia to study the seismicity in and around the Bucaramanga nest. These data are very valuable, because of their low detection threshold (Ml=2.5) and their more accurate location due to application of an improved velocity model (Ojeda & Havskov, 2001) in the process of relocation. Figure 4 shows that due to the low detection threshold, lots of data could be recorded in the small volume of the Bucaramanga nest. The lack of data in some periods is related to technical problem in the seismic network. Figure 5 shows the 3D view of these data.

The existence of two slabs in the area of the Bucaramanga nest is obvious from the local seismicity and it also has been suggested by many other researchers (e.g. Pennington (1981); Van der Hilst & Mann (1994); Ojeda & Havskov (2001)) . The northern slab has a dip angle of $25°$, the dip angle of the slab in the area of the Bucaramanga nest is about $29°$ and in the south the dip of the slab is about $50°$. These observations are generally in agreement with the estimated dip angle for the subducted slabs based on Van der Hilst & Mann (1994). The dip angle of Bucaramanga nest is clearly close to the dip angle of the northern slab. Keeping in mind the existence and geometry of these two slabs, we continued our research with concentrating on the possible reason behind the existence of the Bucaramanga nest. In order to explain the nature of the Bucaramanga nest, we first reviewed all proposed mechanisms by other researchers (e.g. Schneider *et al.* (1987); Van der Hilst & Mann (1994); Cortes & Angelier (2005)), which is summarized in the next section.

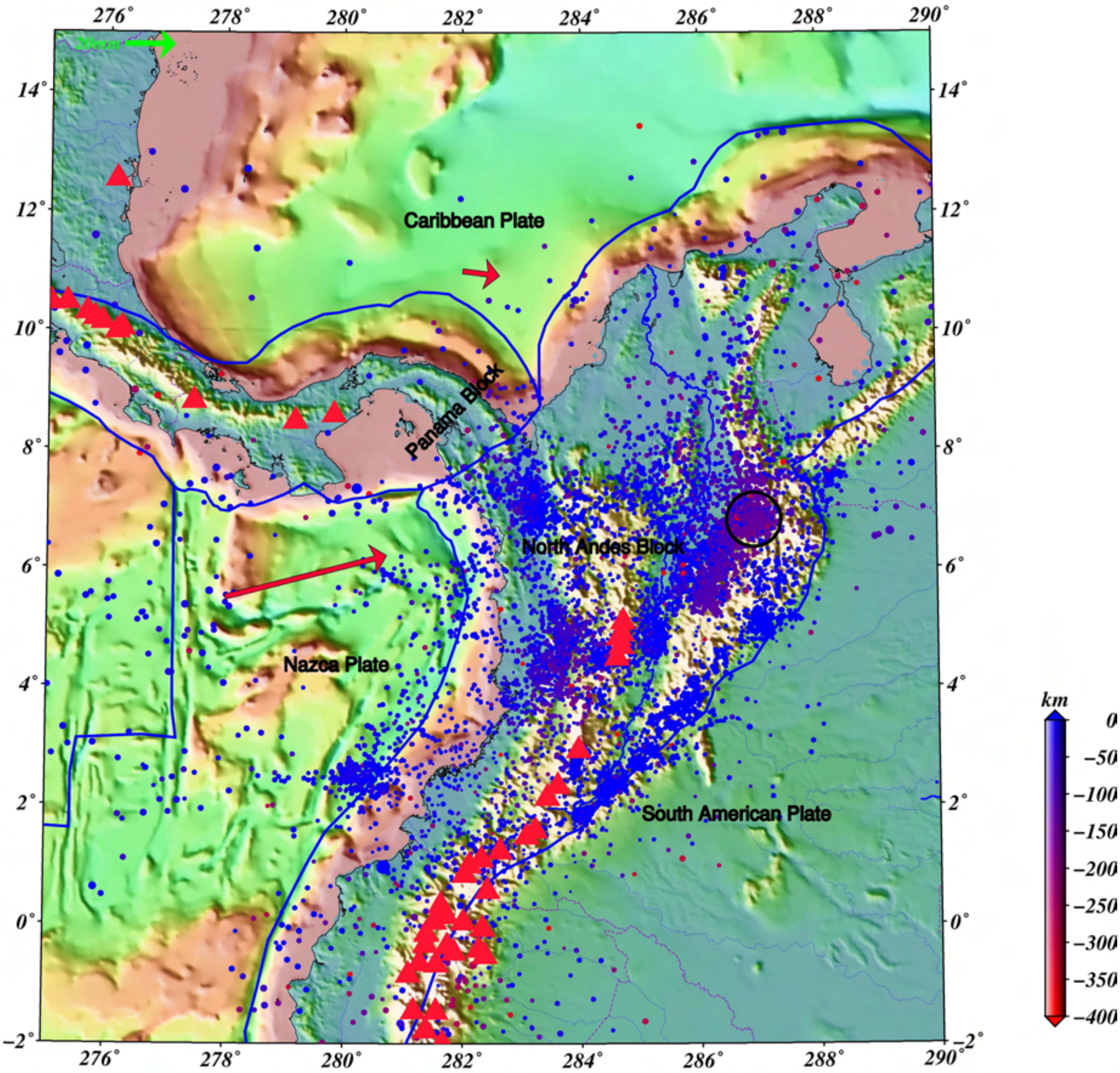

Figure 3: The tectonic setting of Colombia. Seismicity is based on the National Seismic Network of Colombia. The open black circle shows the location of the Bucaramanga nest. The triangles are the location of active volcanoes. Plate boundaries are based on Bird (2003) and velocity of convergence is based on NUVEL-1 model (De Mets *et al.*, 1990).

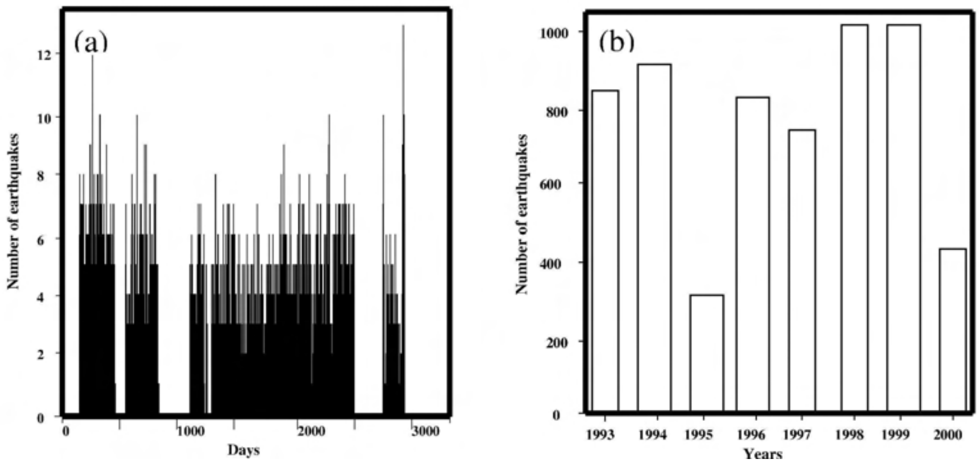

Figure 4: The (a) daily and (b) yearly distribution of the earthquakes inside the Bucaramanga nest.

2.7. The Bucaramanga nest and proposed mechanisms behind its nature

There are different views about the physics behind the existence of the Bucaramanga nest. It was Schneider *et al.* (1987), who, for the first time, studied the mechanism of micro earthquakes inside the Bucaramanga nest and related the variation observed in the stress field to fluid migration. Years later, Van der Hilst & Mann (1994) showed a tomographic image of the two slabs with two different dip angle in the area of the Bucaramanga nest. They believed that Bucaramanga was located in the southern slab with a steeper dip angle. They observed a low velocity zone, below the Bucaramanga nest, in the mantle wedge and they related this observation to the possible scenario for existence of the Bucaramanga nest described before by Schneider *et al.* (1987). However, according to Van der Hilst & Mann (1994), the Bucaramanga nest may also be produced by complex stress field near the contact of the southern and northern slabs. On the other hand Chen *et al.* (2001), proved that there is no correlation between fluid migration, volcanism and intermediate depth earthquakes in Colombia. Also, no volcanic activity can be observed around the Bucaramanga nest. So, the idea of a complex stress field in the area of the Bucaramanga nest received more credit. Cortes & Angelier

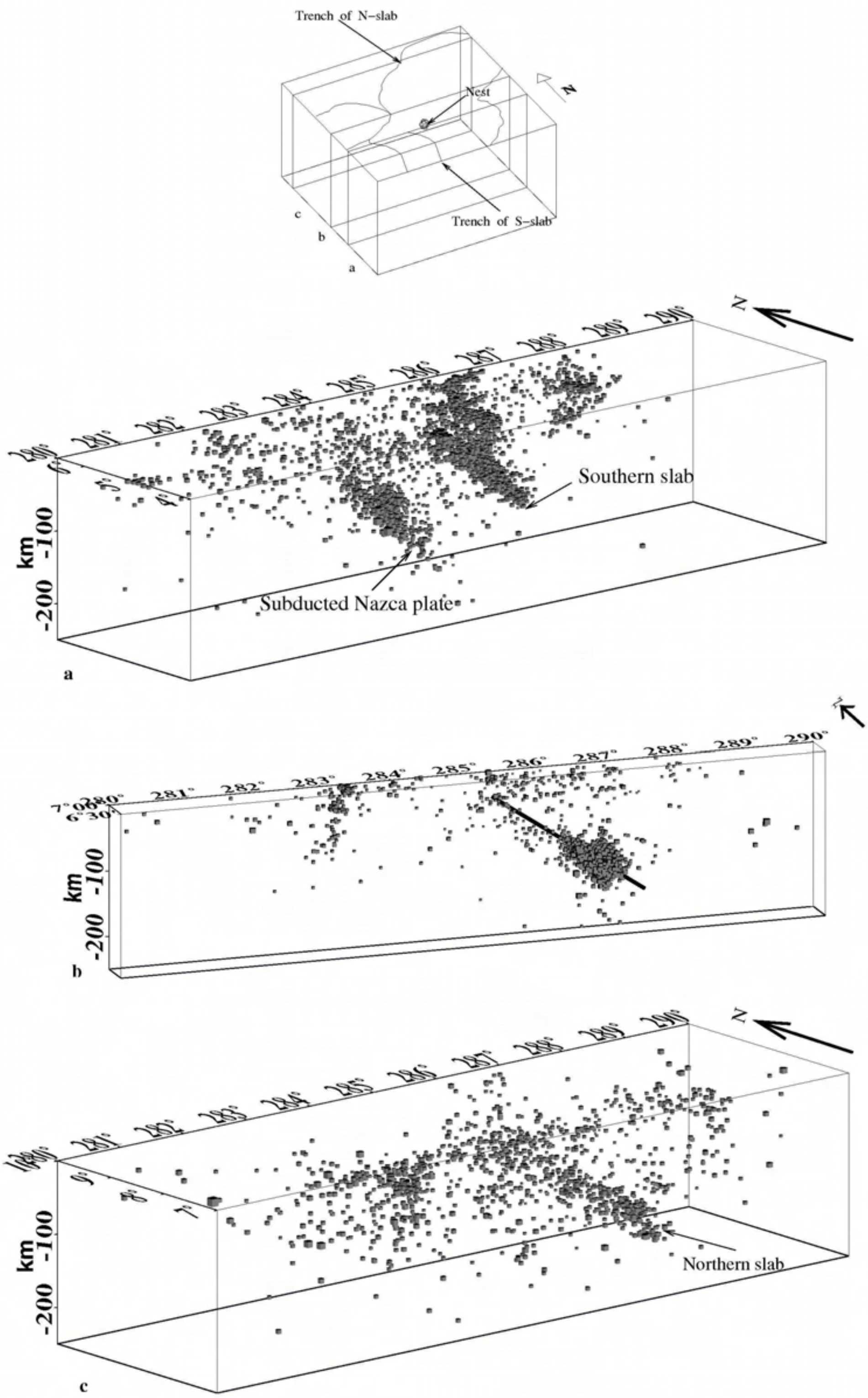

Figure 5: 3D sections of local seismicity in Colombia. The index shows the location of the 3D sections. (a) the southern slab, (b) the Bucaramanga nest and (c) the northern slab. The line in the Bucaramanga nest shows the dip angle of the Bucaramanga nest.

(2005) related this concentrated stress field to the process of slab break-off. However, comparing the Bucaramnga nest with a clear example of slab break off, the Vrancea nest in Romania, does not show consistency. The variation in the mechanism of earthquakes cannot be observed in the Vrancea. Also, the seismicity in the surrounding area of the Bucaramanga nest is not present in the Vrancea. The observed high percentage of CLVDs (based on Harvard CMT solution) in Colombia can not be seen in the Vrancea nest, however the high percentage of CLVDs are also present in the Hindu Kush nest. Existence of CLVDs in the nest is representative of complexity in the source of the earthquakes. Normal faults, which can be observed in the Bucaramanga nest, are not the expected mechanism for the earthquakes at intermediate depth (Richardson & Jordan, 2002). It has been explained that the normal faults at intermediate depth, indicating the final stages of a mature cycle of earthquake in a strongly coupled subduction zone (Dmowska *et al.*, 1988; Taylor *et al.*, 1996; Zheng *et al.*, 1996). However, the low velocity of convergence (1.4 cm/yr (Freymueller *et al.*, 1993)) in the northern slab and the steep dip angle of the southern slab prevent strong coupling in the slab interface (Ruff, 1989; Taylor *et al.*, 1996) and consequently cannot explain the observation of normal faults at intermediate depth. As a result, we propose a different possible nature for the existence of the Bucaramanga nest, which can explain the concentration and variation of the stress field. In the next section, we investigate how collision between two slabs can explain the nature of the Bucaramanga nest.

2.8. Collision between two subducted slabs - a possible explanation for the existence of the Bucaramanga nest

Using the traces of the trenches and the local seismicity in the northeast of Colombia, we constructed a 3D model of the slabs in this part of the north Andes block. These two slabs meet each other approximately at 155 km depth, which is the depth of the Bucaramanga nest. Our constructed 3D model is in good agreement with the schematic

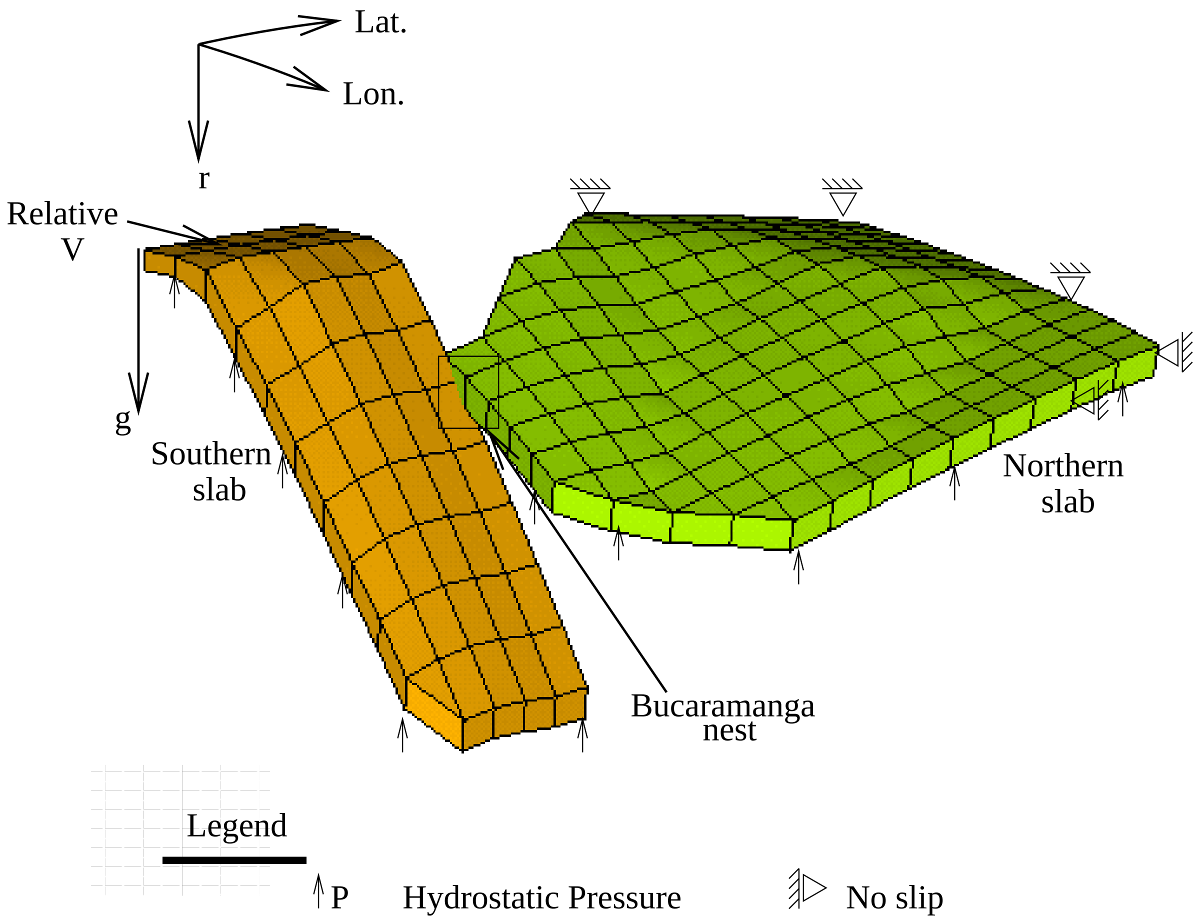

Figure 6: Schematic model and the boundary conditions in the FE model. P is the hydrostatic pressure and g is the gravitational acceleration. The northern slab is considered to be stationary and the southern slab is subducting with the relative velocity between the two slabs.

block diagram obtained by Van der Hilst & Mann (1994) based on tomographic images. Figure 6 shows our constructed model.

We made a 3D FE model using Ansys-ED (2005) to simulate the collision between two elastic slabs, one of which (the northern) is stationary comparing to the other. The southern slab is subducting with the relative velocity between these two plates. These two slabs meet eachother in the area of the Bucaramanga nest and experience frictional sliding in the contact zone. The mantle is considered to be an inviscid Newtonian fluid, so the action of viscous drag on the lithosphere is ignored. Based on this assumption, the effect of the mantle has been constrained to the hydrostatic pressure applied to the lithosphere, where they are in contact (Hassani *et al.*, 1997). For the elastic lithosphere we solved the equation of equilibrium and Hooke's equation. The stress-strain state of an elastic body is described as below (Shemenda, 1994):

$$\sigma_{ij} = E\nu/(1+\nu)(1-2\nu)I_1(\epsilon)\delta_{ij} + E/(1-\nu)\epsilon_{ij}, \tag{1}$$

where, ϵ_{ij} is the strain tensor, $I_1(\epsilon) = \epsilon_{ij}\delta_{ij}$ is the first invariant of the strain tensor, E and ν are the moduli of elasticity and the Poisson ratio. The increase in weight of the slab at 100 km and 300 km depth have been considered due to the amphibolite to eclogite and olivine to spinel phase changes respectively (Lin & Van Keken, 2005). The net balance between the gravitational forces and the hydrostatic pressure of the fluid mantle is calculated based on equation (2) (Marotta & Mongelli, 1998):

$$F_{net} = \delta\rho g S cos(\theta), \tag{2}$$

where $\delta\rho$ is the difference in density between the lithosphere and mantle, S is the thickness of the lithosphere and θ is the dip angle of the subducted lithosphere. We also considered Coulombs friction law in the contact zone of the two slabs (3), changing the coefficient of friction (μ) we found out that the magnitude of stress build up in the contact zone would be changed. We present our result by assuming $\mu = 0.5$. Based on Coulombs' law:

$$\tau = \mu\sigma_n, \tag{3}$$

where τ is the yield stress and σ_n is the normal stress. The elastic thickness of lithosphere has been considered in our modelling (McNutt & Menard, 1982). We monitored the collision for 10000 years (maximum relaxation time for the oceanic lithosphere (Turcotte

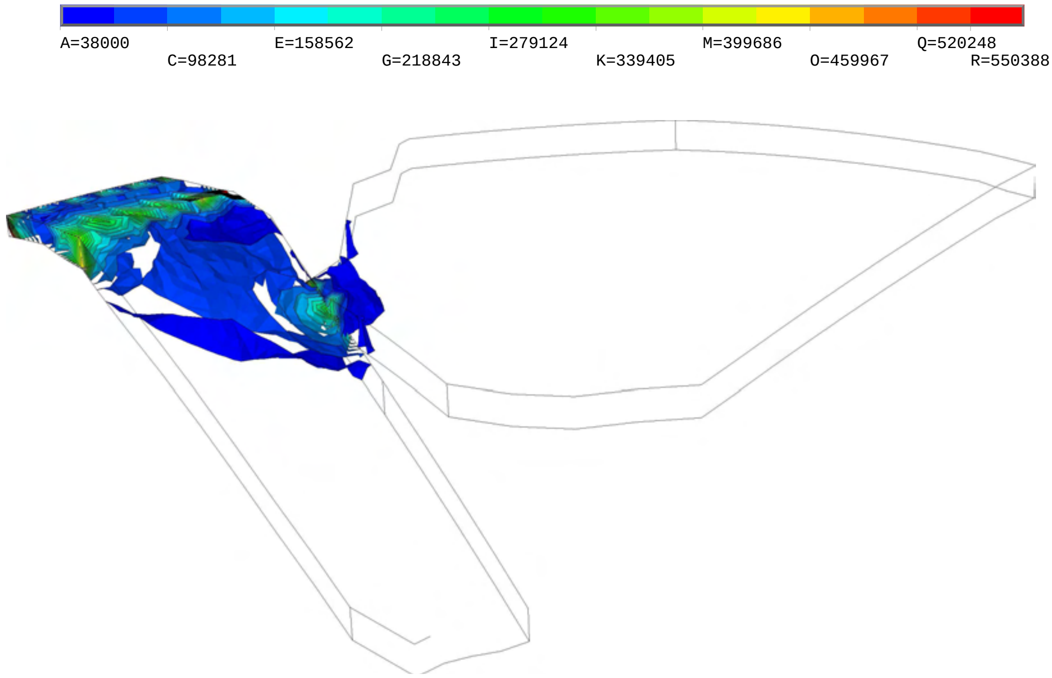

Figure 7: Volume distribution of von Mises stress in the location of collision between the two slabs (the Bucaramanga nest).

& Schubert, 2002)). The results show (Figure 7 and 8) how collision can concentrate and modify the stress field and may explain the nature of the Bucaramanga nest.

We conclude that the dehydration reaction at intermediate depths can lower the strength of the lithosphere and the concentrated stress field in the collision zone can give rise to the concentrated seismic activity that is observed in the area of the Bucaramanga nest. The subduction of slab under its own weight and the modified stress field due to the collision can also explain the variation in the mechanism of earthquakes in the Bucaramanga nest. The earthquakes with non-double couple component and away from volcanoes usually are related to the complexity in the source (Aki, 1979). Collision can produce such a complexity in the process of faulting.

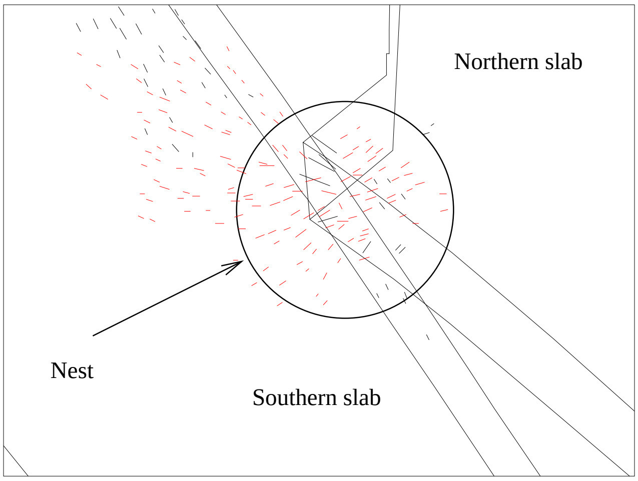

Figure 8: Redrawn sample of tensile and compressional tensors in and around the Bucaramanga nest. The red lines show the compressional and the black lines the tensional stress tensors.

3. Unusual subduction zones- low rate of seismic activity in the slab interface

Some subduction zones do not show frequent seismic activity in the fore-arc setting and this makes it difficult to determine whether they have very strong or very weak coupling in the slab interface. There is ongoing dispute over the type of coupling in Makran, especially in the western part (e.g. Byrne *et al.* (1992); Carayannis (2006); Nowroozi (1971)), which has no seismic activity at present and may have experienced large earthquake in historical times. In the next sections of this research, we study the Makran subduction zone using seismicity, focal mechanism, gravity and FE modelling in order to find a proper explanation for its unusual seismic behavior.

3.1. Makran subduction zone - overview

The Makran subduction zone in the southeast of Iran and southern Pakistan marks a zone of convergence where the oceanic crust of the Oman sea is subducting beneath the Eurasian continent since the early Cretaceous (Farhoudi & Karig, 1977). Makran is bounded to the west by the continent- continent collision of the Arabian and the Eurasian plates and to the east by the continent-continent collision between the Indian and the Eurasian plates (Figure 9). The rate of convergence along the Makran boundary increases slightly from the west towards the east (De Mets *et al.*, 1990). The segmented overriding lithosphere in the Makran consist two blocks, the Lut block in the west and the Helmand block in the east. The volcanoes are situated further north in the eastern part than in the western part of the Makran subduction zone (Figure 10). The relocated data based on Engdahl & Villasenor (2002) show that eastern Makran is subducting with a dip angle of about $8°$, increasing to about $20°$, where it bends into the asthenosphere. The dip angle of the slab in the western Makran where it subducts below the overriding lithosphere is not clear but it bends into the asthenosphere with a dip angle of about $30°$. We examined the free air gravity anomaly perpendicular to the trench in the eastern and the western Makran and the results show that the gravity anomaly in the trench area in the western Makran is more negative compared to the east. This means that the dip angle of the slab where it subducts beneath the overriding lithosphere is steeper in the west compared to the east.

The present day seismicity in Makran is spars. Moderate to large magnitude earthquakes are either related to the down going slab at intermediate depths or superficial in the eastern Makran (e.g. 1765, 1851 and 1945 earthquakes), while western Makran is marked with almost no seismicity in the coastal area at present but might have experienced a strong earthquake in 1483 (Ambraseys & Melville, 1982; Byrne *et al.*, 1992), however there is no solid proof for that (Figure11). Page *et al.* (1979) have suggested that the presence of young marine terraces along parts of the western Makran, in Jask and Konarak (Figure 11), provides strong evidence for the occurrence of great thrust earthquakes in the fore-arc setting of the western Makran. However, other researchers believe that the processes of formation of marine terraces is disputable and might not necessarily be related to the occurrence of thrust earthquakes (Fitch & Scholz, 1971;

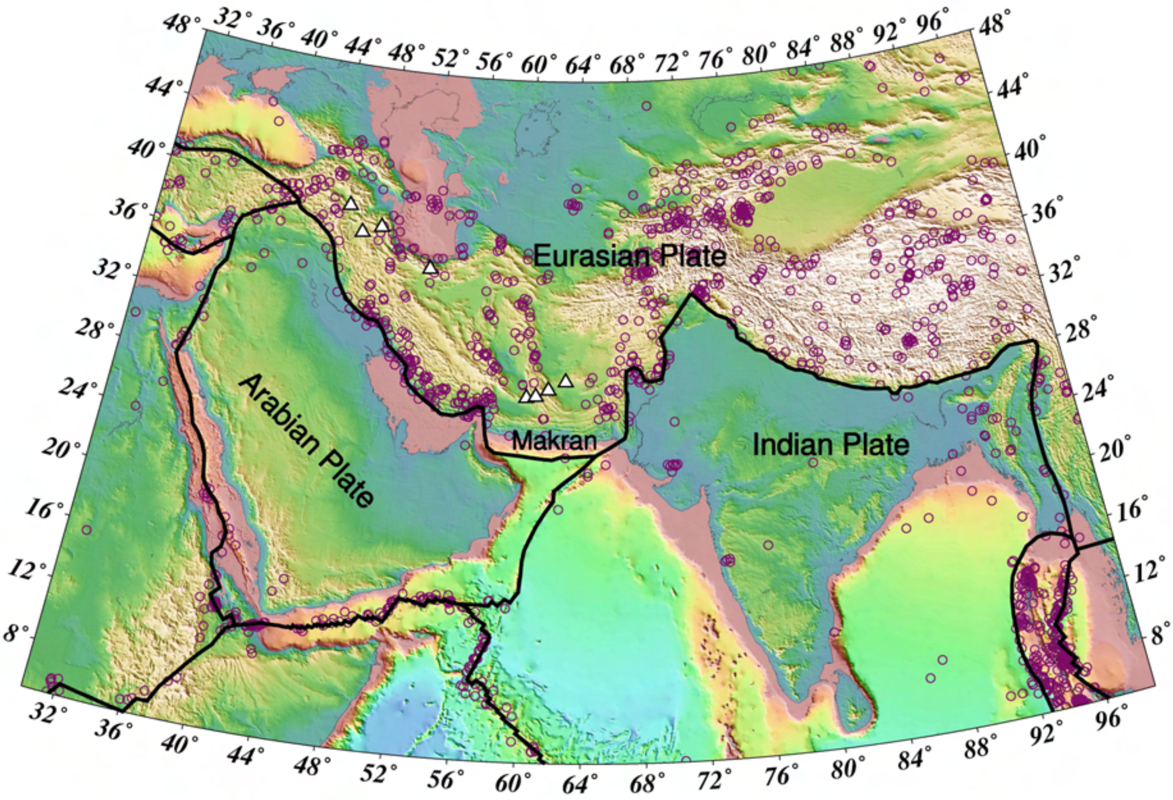

Figure 9: Makran is bounded on the west by the continent-continent collision between Arabia and Eurasia and on the east with the continent-continent collision between India and Eurasia. The purple circles show the seismicity for earthquakes with $M_w > 5.0$ from Harvard catalog (1976- present). The solid thick black line represents the plate boundary based on Bird (2003).

Byrne *et al.*, 1992).

Observation in eastern Makran shows that the rate of seismicity in the westernmost of the 1945 earthquake ruptured zone has been increased (Quittmeyer & Jacob, 1979). This area almost corresponds to the easternmost of the rupture zone of the 1851 earthquake and there is speculation about recurrence of a future earthquake in this area (Byrne *et al.*, 1992; Carayannis, 2006). Makran has experienced a Tsunami after the 1945 earthquake (Byrne *et al.*, 1992; Carayannis, 2006), and probably this was not the first tsunami experienced in the Makran subduction zone. There are some indications that the 1765 earthquake was also followed by a tsunami (Ambraseys & Melville, 1982).

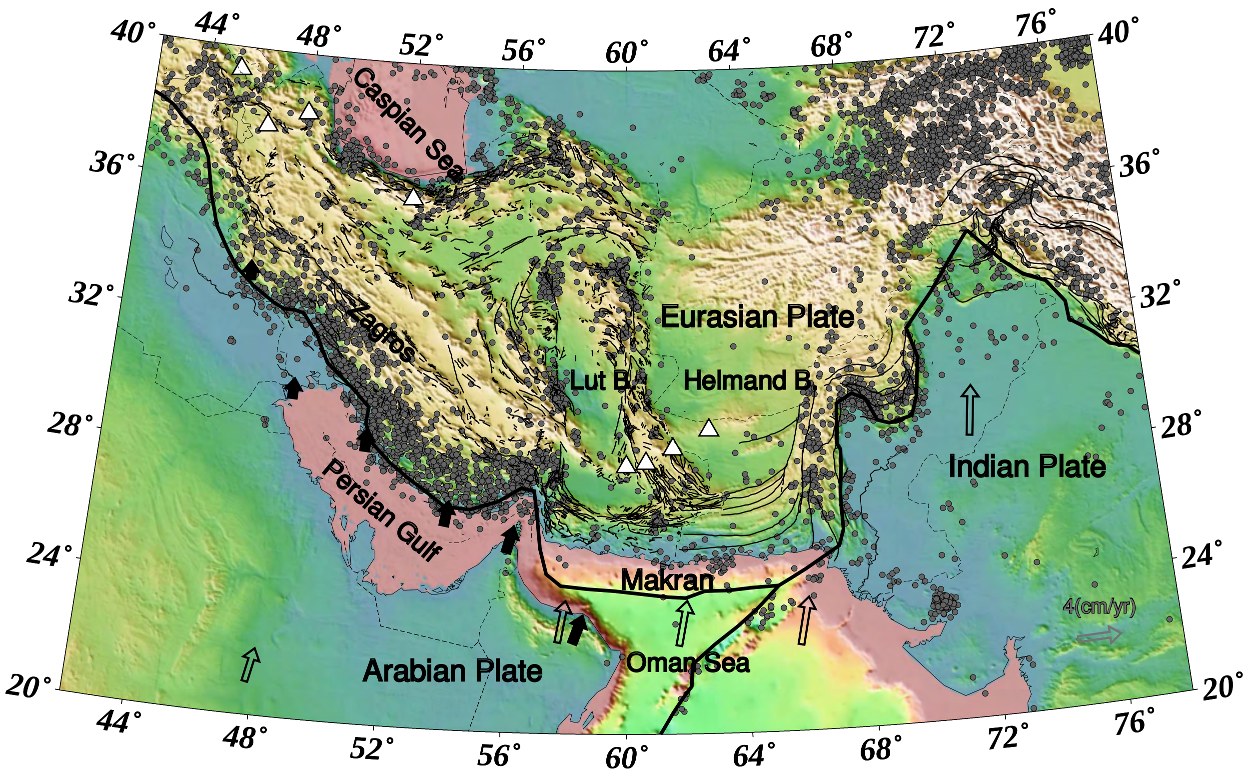

Figure 10: A general view of the Makran subduction zone and its surroundings. The solid black arrows show the direction and magnitude of convergence based on GPS observation (Nilforoushan *et al.*, 2003). The open black arrows show the convergence velocity based on NUVEL-1 (De Mets *et al.*, 1990). The white triangles show the location of volcanoes. The seismicity is based on ISC catalog ($M_b \geq 4.5$).

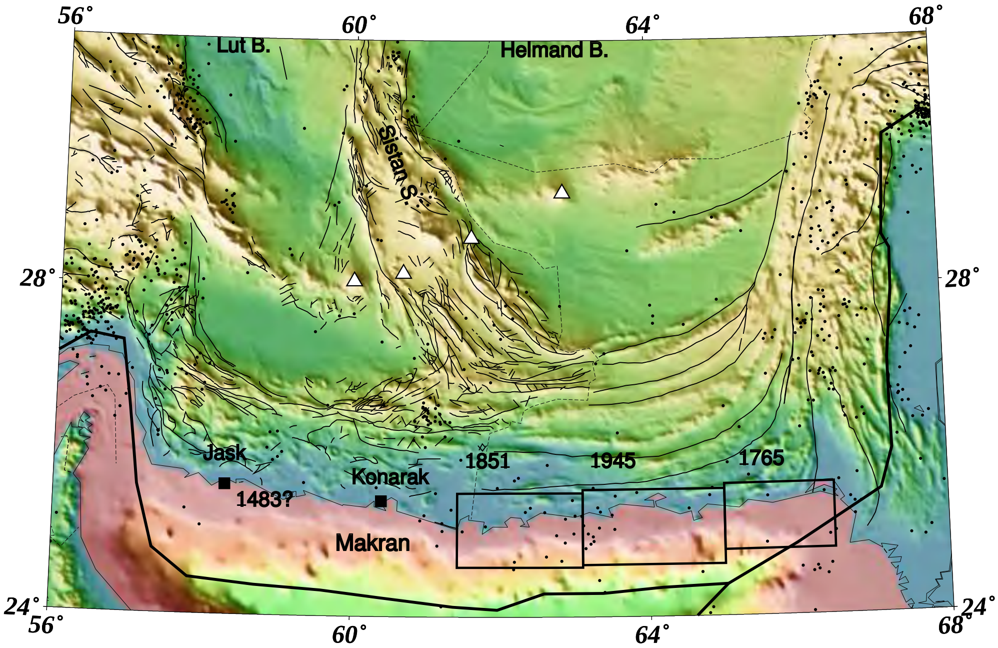

Figure 11: Ruptured area of strong earthquakes in the eastern Makran based on (Byrne *et al.*, 1992). Jask and Konarak are the site of observed marine terrace in the western Makran (Page *et al.*, 1979).

Therefore understanding the seismogenic behavior of the Makran subduction zone is important.

The aim of this research is to better understand the state of stress in the overriding lithosphere in Makran and the influence of the collision zones on the Makran stress field. We also try to provide a good understanding about the seismogenic behavior of the slab interface in the Makran subduction zone. We explain how the overriding lithosphere experiences deformation within a cycle of earthquake. These are discussed in detail in papers 3 and 4.

3.2. Current state of crustal stress in Makran - focal mechanism stress inversion

For the details of this study please refer to paper 3

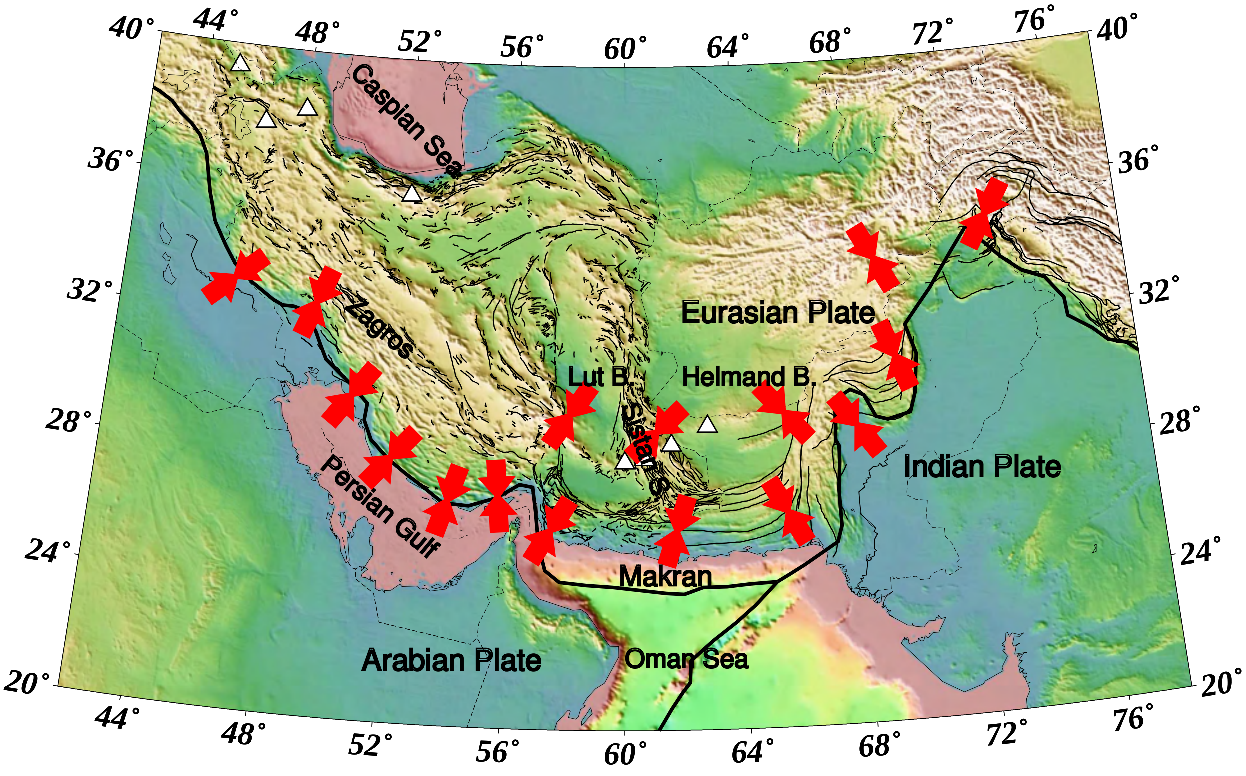

Figure 12: The maximum horizontal-compressional stress obtained from the focal mechanism stress inversion. Clearly the state of stress is changing from the western to the eastern Makran. The western Makran stress field is under the influence of the stress field associated with the collision zone between Arabia and Eurasia, while the eastern Makran stress field is influenced by the Indian-Eurasian stress field.

We used the focal mechanism of shallow earthquakes (depth < 45 km) in Makran and also in the collision zones between the Arabian-Eurasian and Indian-Eurasian plates to study the current state of stress in the region. The aim is to investigate the state of stress in the overriding lithosphere in Makran and to observe any possible influence of the collision zones on the Makran stress field. The sources of data are mainly Harvard CMT solutions, but in the Maktran region, we also used other published focal mechanisms for the earthquakes (e.g. Byrne *et al.* (1992); Dziewonski *et al.* (1983); Quittmeyer & Kafka (1984)). We used an approach based on the Michael (1984, 1987*a*,*b*) and Michael (1991) method to determine the spatially uniform time averaged component of the stress field in the region. The final result of stress inversion show that the direction of compressional stress axis is rotating along the Makran subduction zone. The western Makran stress field is under the influence of the collision between Arabia and Eurasia, while the eastern Makran stress field is affected by Indian-Eurasian collision. Figure 12 shows the direction of the compressional stress axis in the entire region. The variance of inversion everywhere is less than 0.17, suggesting appropriate fit with a homogeneous stress field. The maximum variance is associated with the Makran region, which may be related to uneven source of data that has been used here.

3.3. Source analysis of intermediate depth earthquakes around the Sistan suture zone

For the details of this study please refer to paper 3

We analysed the source and the mechanism of three recent intermediate depth earthquakes around the Sistan suture zone using body wave inversion. The Sistan suture zone connects the two segmented blocks, Lut and Helmand, on the overriding lithosphere (Figure 11). It is believed that the Sistan suture zone provides evidence for subduction of part of the Neo-Tethys to the east beneath the Helmand block when these two blocks

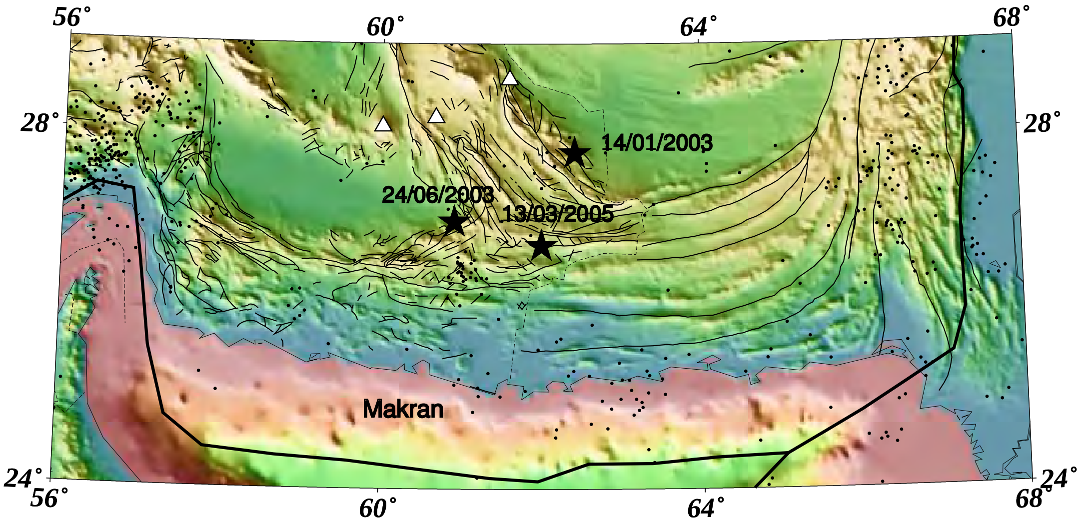

Figure 13: Location of the three intermediate depth earthquakes, which occurred recently in the Makran slab and around the Sistan suture zone.

were once separated (Tirrul *et al.*, 1983). Our main concern is to know whether the Sistan suture has a thick root and may meet the Makran slab at intermediate depths. In general we look for complexity in the source of the earthquakes in the area around the Sistan suture zone. Figure 13 shows the location of the recent earthquakes that we studied in this research. Depth of earthquake in 14/01/2003 is about 80 km. The 24/08/2003 earthquake occurred at 72 km depth and the last earthquake in 2005 occurred at 58 km depth.

In order to do body wave inversion we used the Kikuchi & Kanamori program (Kikuchi & Kanamori, 2003) and the Broad Band P and SH waves from stations of the Incorporated Research Institutions for Seismology (IRIS). To avoid the upper mantle triplication and interference from the core phases, waveforms in the distance range of $30° - 75°$ have been used (Maggi *et al.*, 2000). The amplitude of P and SH waves are corrected for the effect of geometrical spreading and attenuation by adopting t^* value of 1.0 s for P waves and 4.0 s for SH waves. t^* is the travel time divided by the quality factor in a region of uniform attenuation. We used the spherical average velocity structure based on the

AK135 model (Montagner & Kennet, 1995) and a rupture velocity of 3 km/s. In the process of inversion, the weight of P waves is 10 times more than that of SH waves. The result of body wave inversion shows no source complexity for the two earthquakes at 80 and 72 km depth, however the earthquake at 58 km depth (on 13/03/2005) has a complex source (Figure 14a,b). The result is comparable with the Harvard CMT solution for this earthquake, which shows more than 50% non-double couple component. This may indicate that at intermediate depths around 58 km, there is a source of complexity. This may be related to the thick root of the Sistan suture zone, which meets the low dip angle slab at that depth and produce the source of complexity. However, this is just an indication and cannot be confirmed without a detail tomographic investigation.

3.4. Western Makran as a strongly coupled segment of the subduction zone

For the details of this study please refer to paper 4

Western Makran does not experience seismic activity at present. The seismogenic behavior of the western Makran, created uncertainty about the type of coupling in this section of slab interface. In the 4th paper we try to show that the only possibility in the western Makran is strong coupling. The following sections explain our observations on our modelling and interpretation of the western Makran.

3.5. Trench Parallel Gravity and Topography Anomaly (TPGA and TPTA)

Recent studies (Song & Simons, 2003; Wells *et al.*, 2003; Hackney *et al.*, 2005) demonstrate that great earthquakes occur predominantly in regions with a strong negative Trench Parallel Gravity and Topography Anomaly (TPGA and TPTA) [TPGA< -40 mGal and TPTA < -750 m]. TPGA and TPTA maps can be constructed by removing

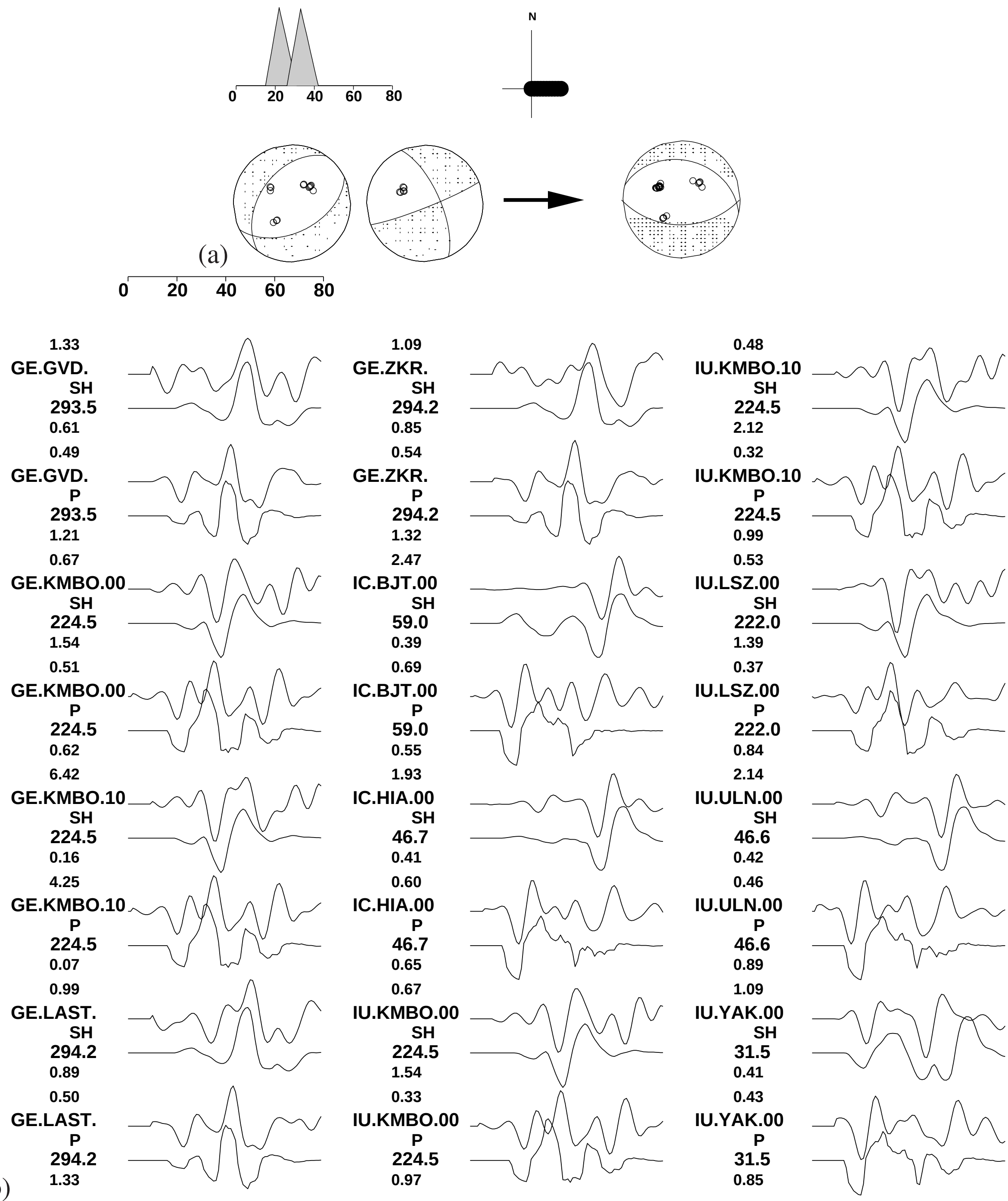

(b)

Figure 14: Result of body wave inversion for intermediate depth (58 km) earthquake of 13/03/2005. (a) Source time function of the event which shows complexity (b) Observed (top) and produced synthetic (bottom) seismograms.

the average of regional gravity anomaly perpendicular to the trench. The reason for making this residual map is to remove the effect of slab buoyancy and mantle rheology from the free air gravity data. The constructed residual map (TPGA map) will then be under the control of shallower structure in the slab interface. The TPTA map usually follows the TPGA map since the free air gravity anomaly has positive correlation with the Topography. Song & Simons (2003) argue that the observed correlation between TPGA and TPTA imply increased shear traction caused by an increase in the static coefficient of friction. This means that in areas with highly negative TPGA and TPTA, the overriding lithosphere is strongly coupled with subducting lithosphere and it is dragged down with the subducting slab. This cause the negative topography and consequently free air gravity anomaly in the fore-arc setting.

3.6. Results and interpretation of TPGA and TPTA in Makran

We construct the TPGA and TPTA map in the fore-arc setting of the Makran subduction zone. Figure 15 shows the result of our investigation. It is obvious that the entire western Makran fore-arc is located in areas with TPGA <-50 mGal and TPTA <-750 m. The western Makran is separated from the eastern Makran with areas of positive TPGA and TPTA. This area is located along the Sistan suture zone in the fore-arc setting. The area of the 1851 and the 1945 earthquakes correspond with the positive TPGA and TPTA, which needs explanation. In general there is a good agreement between the TPGA and TPTA maps everywhere in the fore-arc setting of the Makran subduction zone except for the area of the 1765 earthquake.

Based on other researches (Song & Simons, 2003; Wells *et al.*, 2003; Hackney *et al.*, 2005), which were carried out in the Pacific and the Java, we related the observed negative TPGA and TPTA in the western Makran to a high coefficient of friction in the contact zone (e.g. strong coupling between the overriding and subducting plates) between 14-26 km depth along the slab interface. The depth interval of this strong coupling in

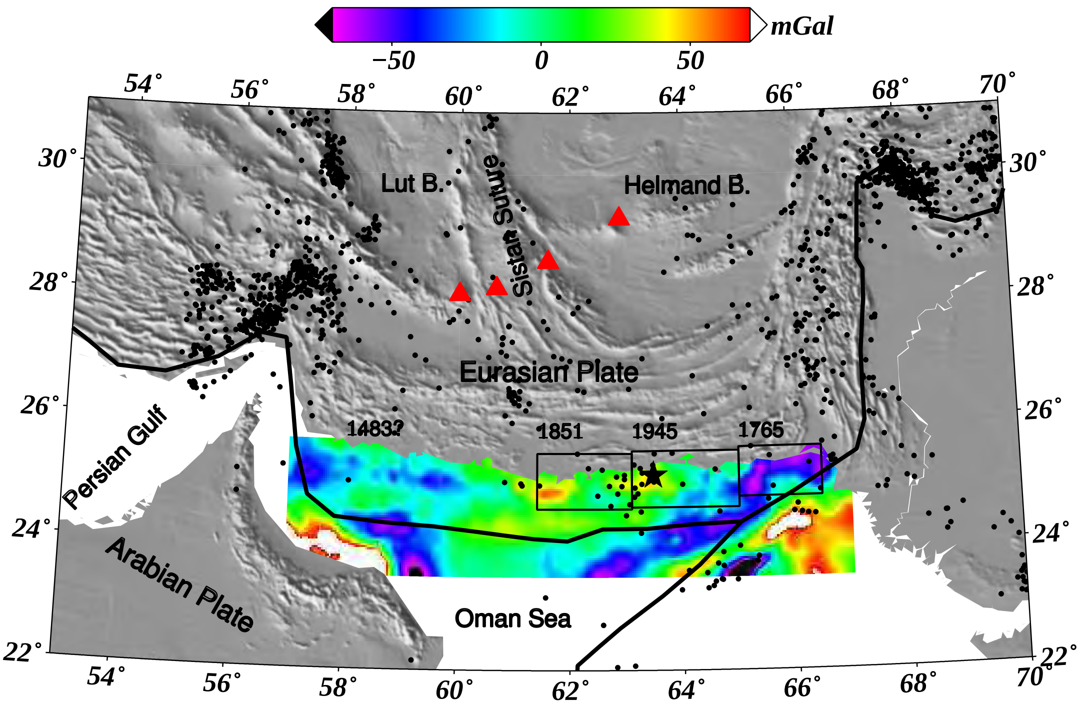

(a)

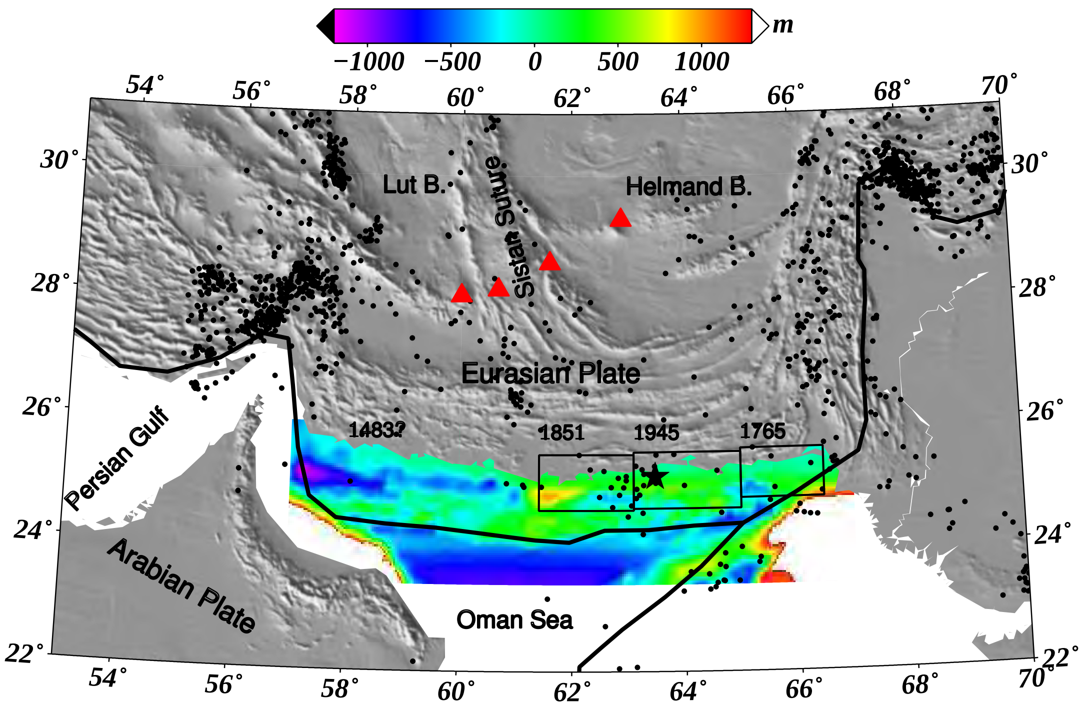

(b)

Figure 15: (a) The TPGA and (b) TPTA map in the Makran fore-arc setting.

the slab interface is estimated based on geometry of the slab, which we obtained from seismicity.

3.7. FE modelling of shear stress build up in the contact interface of the western Makran

We used a 2D elastic-viscoelastic FE model to investigate the rate of shear stress build-up in the slab interface of the western Makran. We considered Coulomb's friction law (equation 3) in the contact zone between the overriding and subducting plates. We changed the coefficient of friction along the slab interface, where the smallest coefficient $(\mu = 0.25)$ corresponds to the shallower part of slab interface and the largest coefficient of friction $(\mu = 0.85)$ belongs to the area of the strongest coupling between 14-26 km depth. Velocity of convergence is based on GPS observation in the western Makran (about 2.6 cm/yr (Nilforoushan *et al.*, 2003)). The lithosphere has a elastic behavior in our model (based on Equation 1) and the mantle act as a viscoelastic material, with the following constitutive equation (Ansys-ED, 2005):

$$\sigma = \int_0^t 2G(\mathrm{t} - \tau)\frac{de}{d\tau}d\tau + I\int_0^t K(t-\tau)\frac{d\triangle}{d\tau}d\tau, \quad (4)$$

where σ is the stress, e is the deviatoric part of the strain, $\triangle$ is the volumetric part of the strain, $G(t)$ is the shear relaxation kernel function, $K(t)$ is bulk relaxation kernel function, t is the current time, τ is the past time and I is the unit tensor. The kernel functions are represented in terms of Prony series which assumes that:

$$G = G_\infty + \sum_{i=1}^{n_G} G_i \exp(\frac{-t}{\tau_i^G}), \quad (5)$$

$$K = K_\infty + \sum_{i=1}^{n_K} K_i \exp(\frac{-t}{\tau_i^K}), \quad (6)$$

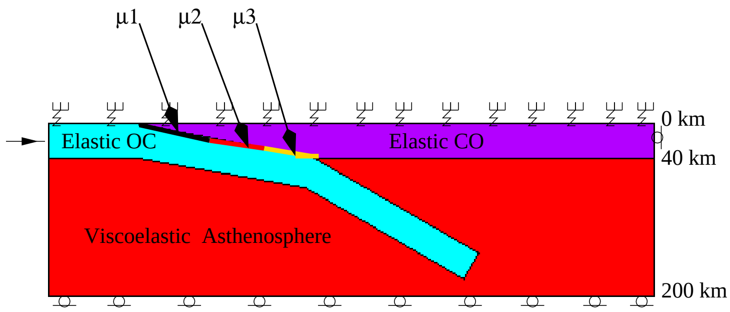

Figure 16: Geometry and boundary condition of the mechanical model in the western Makran.

where G_∞ and G_i are shear elastic moduli, K_∞ and $K_i$are bulk elastic moduli and τ_i^G and τ_i^K are the relaxation times for each Prony component. The model used in the western Makran is presented in Figure 16.

The result of modelling shows that the processes of shear stress build up in the contact zone is very slow. It takes almost 1400 years until the shear stress in the strongly coupled part of the slab interface reaches the yield point. However, this calculation cannot be the representative of the recurrence time for an earthquake, since we did not consider any complexity regarding the frictional behavior, pre existing stress or loading due to occurrence of other earthquakes in this segment of subduction. Figure 17 shows the result of numerical modelling.

3.8. Makran and mature stages of an earthquake cycle

For the details of this study please refer to paper 4.

Normal faults are the dominant mechanism of earthquakes at intermediate depths in the Makran subduction zone (Figure 18). These earthquakes are mainly concentrated in the area at intermediate depths, which corresponds to the rupture zone of the 1851 earthquake in the fore-arc setting and also in the western Makran. The existence of normal fault mechanism at intermediate depths has been explained first by Dmowska *et al.*

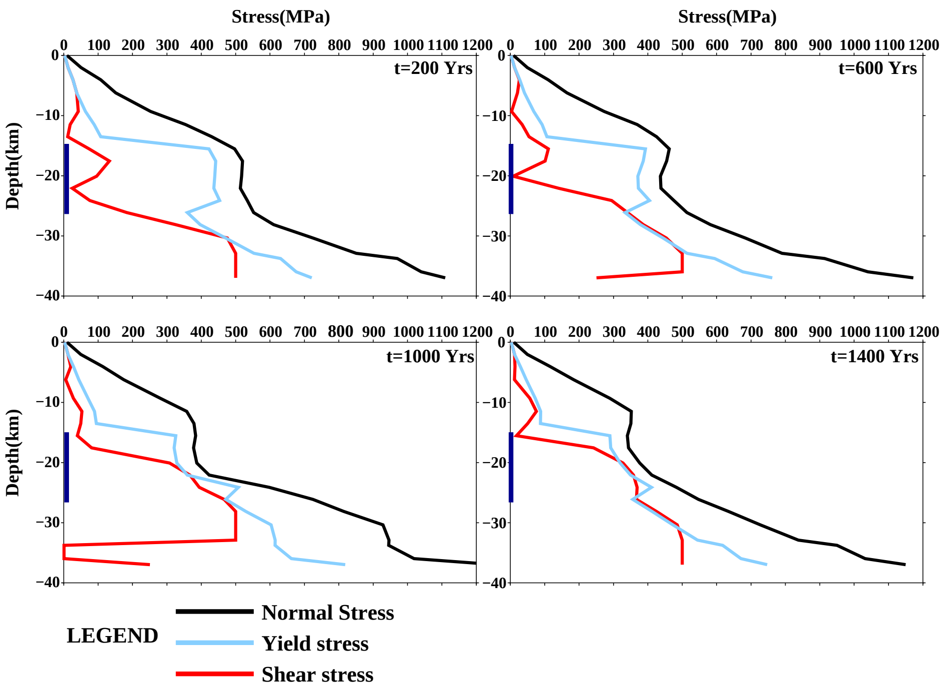

Figure 17: Result of FE modelling in the western Makran. The depth range of strongly coupled segment is shown by the dark blue line.

(1988) using a 1D Finite Element (FE) model and later has been developed further with a 2D FE model by Taylor *et al.* (1996). Dmowska *et al.* (1988) suggested that "the direct evidence of tensional stress acting on the down going slab in the latter portion of the earthquake cycle, at depths starting from just below the zone of thrust earthquakes (about 40 km depth) and reaching to 200-250 km depth, is the occurrence of earthquakes with a normal mechanism in many zones around the world. Such intermediate term precursory shows that this particular part of the subduction zone entered the mature stage of an earthquake cycle". Dmowska *et al.* (1988), Taylor *et al.* (1996) and Zheng *et al.* (1996), argued that depending on the degree of coupling, the coupled part of the slab interface undergoes periodically repeated large slip of $\alpha V_{pl} T_{cyc}$, where α is the seismic coupling factor (the ratio of sudden slip in earthquake to total slip within a cycle), V_{pl} is the velocity of convergence and T_{cyc} is the time period of one cycle. They assumed that the remaining part of $(1-\alpha)V_{pl}T_{cyc}$ of total convergence $V_{pl}T_{cyc}$ in a cycle is accommodated by sliding at constant rate of $(1-\alpha)V_{pl}$, which is the sliding rate in modelling of

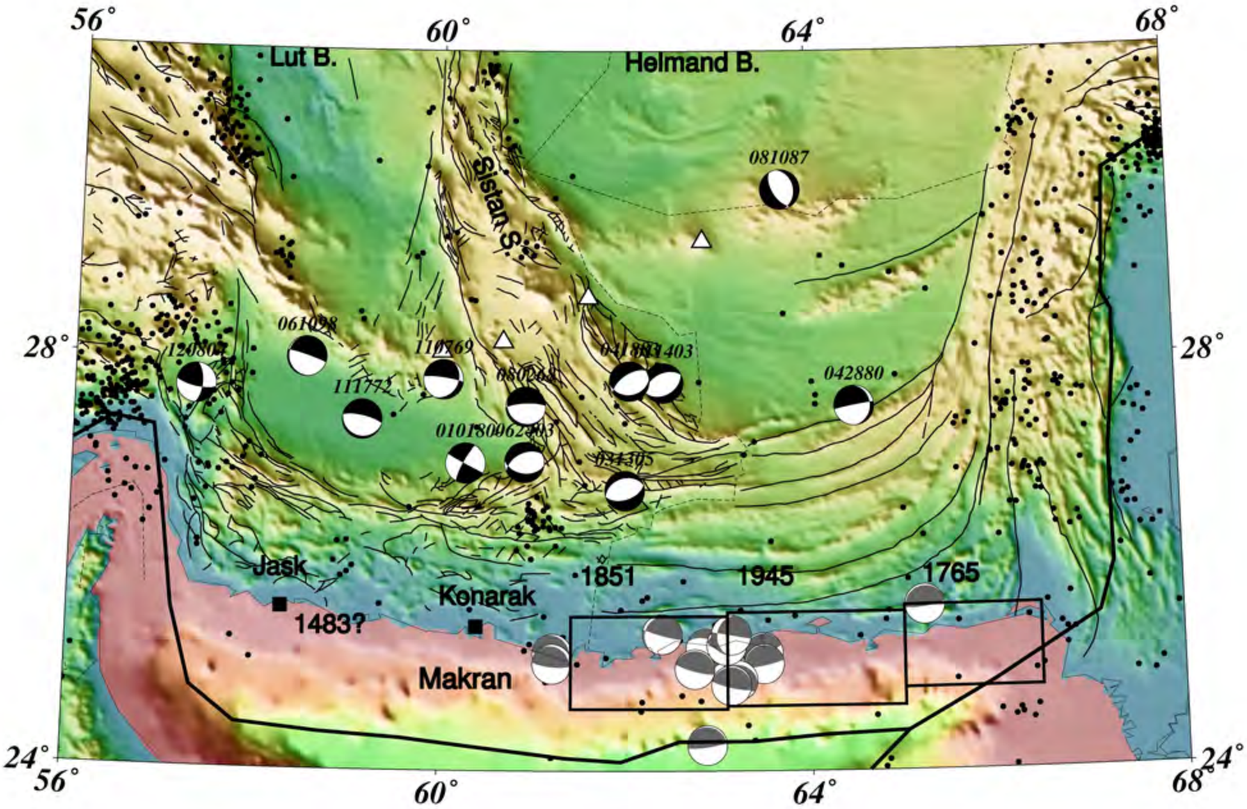

Figure 18: Mechanism of shallow earthquakes (gray) in the fore-arc setting and intermediate depth (black) in the Makran subduction zone. The rectangles are the rupture zone of large earthquakes in the eastern Makran based on Byrne *et al.* (1992). Jask and Konarak are the site of observed marine terraces in the western Makran.

earthquake cycle.

According to Zheng *et al.* (1996) The preconditioning slip history, up to and including a large earthquake is expressed as:

$$\triangle u = (1-\alpha)V_{pl}t + \{\frac{1}{2} + [\frac{t}{T_{cyc}}]\alpha V_{pl}T_{cyc}\}, \quad (7)$$

where $\triangle u$ is the slip, t is time and $[\frac{t}{T_{cyc}}]$ is a staircase function. Based on Taylor *et al.* (1996), the slip can be separated into two parts, the steady slip and the perturbation slip, as $\triangle u = \triangle u_{steady} + \triangle u_{perturb}$ with $\triangle u_{steady} = V_{pl}t$, and

$$\triangle u_{perturb} = \{\frac{1}{2} + [\frac{t}{T_{cyc}}] - \frac{t}{T_{cyc}}\}\alpha V_{pl} T_{cyc}, \tag{8}$$

where $\triangle u_{perturb}$ averages, in time, to zero over one whole seismic cycle and is associated with the temporal variation in coupling (Zheng *et al.*, 1996; Taylor *et al.*, 1996). This term drives the time dependencies of deformation in the overriding lithosphere above the slab interface which can be monitored by geodetic observations (Zheng *et al.*, 1996). We use the $\triangle u_{perturb}$ as a load on the slab interface, when we model deformation in the overriding lithosphere within a cycle of earthquake.

3.9. FE modelling of deformation in the overriding lithosphere within an earthquake cycle

The source of the 1945 earthquake in the eastern Makran has been studied by Byrne *et al.* (1992). According to that study the average slip associated with the 1945 earthquake was about 6-8 m. The 1851 earthquake had a magnitude slightly less than the 1945 earthquake (Byrne *et al.*, 1992). Therefore, we used the fault geometry and the minimum slip associated with the 1945 earthquake as an input to model the deformation within a cycle of earthquake in the overriding lithosphere. This modelling can help us to estimate and compare the rate of deformation in the overriding lithosphere above the segments associated with the 1945 and the 1851 earthquakes.

Since we don't have any clue about the length of earthquake cycle in the eastern Makran, we used three cycles of earthquakes in our modelling. The length of cycles is 200, 250 and 300 years. Following research by Zheng *et al.* (1996) in the Shumagin subduction in Alaska, we considered a heterogeneous coupling in the slab interface and associated the maximum local coupling factor to the ruptured length of the 1945 earthquake. The seismic coupling factor is changing locally, with the ratio of 1.5:3:2.5 , where 1.5 is along the shallow aseismic segment of the slab interface, 3 is associated with the rupture length of the 1945 earthquake and 2.5 is associated with the area below the rupture zone

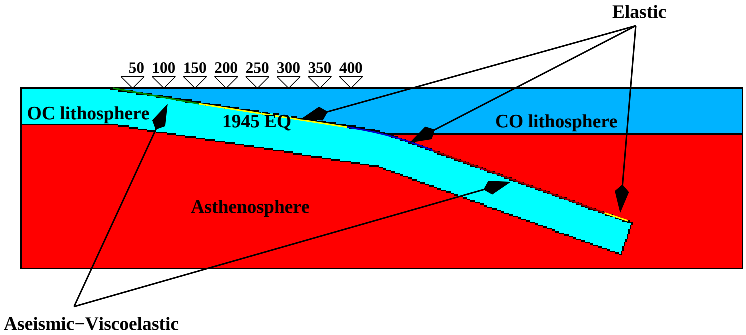

Figure 19: Model of the eastern Makran used in this study. The geometry of the slab is based on the observed seismicity.

of the 1945 earthquake in the slab interface. The seismic coupling factor α is 0.70 for $T_{cyc} = 200$ years, 0.56 for $T_{cyc} = 250$ years, and 0.48 for $T_{cyc} = 300$ years. Using a 2D elastic-viscoelastic model, where load in the slab interface considered to be $\triangle u_{perturb}$ for the local value of α, we found the deformation in the overriding lithosphere within a cycle of earthquake. In our model, the aseismic portions of the slab are considered to be viscoelastic (based on Equations 4, 5 and 6) with a short relaxation time, to avoid any stress build up in those portions. These portions are between 0-17 km and 80-110 km. The rest of the lithosphere is elastic (based on equation 1) and the mantle reacts as a viscoelastic material. The model is presented in Figure 19.

Figure 20 shows that in the beginning of the cycle the overriding lithosphere experiences uplift, in the middle of the cycle no deformation can be associated with the overriding lithosphere and close to the end of the cycle, the overriding lithosphere is experiencing subsidence. The deformation is more pronounced in a distance of 200-350 km away from the trench where it is associated with the strongest coupling in the slab interface. Considering different lengths for the cycle of earthquake, we could observe that the rate of deformation is faster, when the length of cycle is shorter.

We also compared the present state of deformation in the segments of the 1945 and the

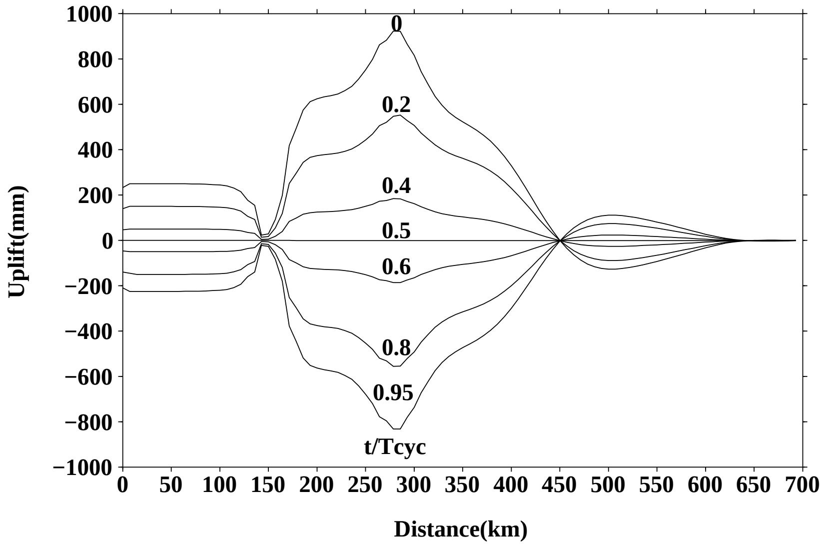

Figure 20: Vertical displacement away from the trench (0 distance) for different time within a cycle of earthquake with 200 years length. The maximum vertical displacement is associate with the area above the strongly coupled segment of the slab interface.

1851 earthquakes (Figure 21) for different cycles of earthquake. Clearly if the cycle of earthquake is 300 years, we should observe very little deformation at the present time in the overriding lithosphere above the 1851 earthquake. That is because the segment would be almost in the middle of earthquake cycle. This cannot be the case in this segment. The concentrated normal faults show the induced extensional stress at intermediate depths in this segment. According to Taylor *et al.* (1996), this induced stress would be almost zero in the middle of cycle, and no normal faulting should be observed at intermediate depths. So 300 years length for cycle of an earthquake with almost the same magnitude of 1851 is quite long. It also means that the area of 1945 earthquake may be reactivated in a shorter time compared to 300 years that has been proposed by Byrne *et al.* (1992).

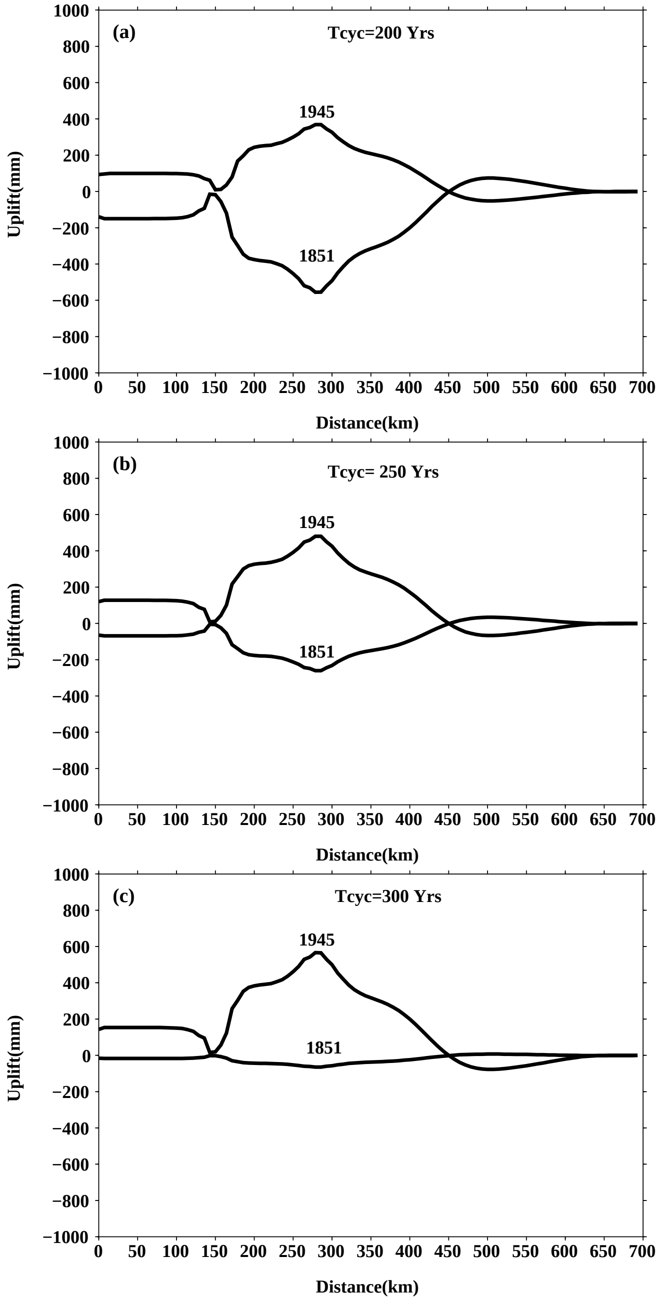

Figure 21: The comparison between the present day deformation in the overriding lithosphere above the rupture zones of the 1945 and the 1851 earthquakes for (a) $T_{cyc} = 200$ (b) $T_{cyc} = 250$ and (c) $T_{cyc} = 300$ years.

4. Discussions

The main characteristics of earthquake nests reveal that they are associated with concentration of the stress field in a small volume. They occur as a result of long term tectonic process, which can be due to slab break off (e.g. the Vrancea nest), collision between subducted slabs (e.g. the Bucaramanga or Hindu Kush nests) or an abrupt change in the geometry of the subducted slab (e.g. the possible nest in Fiji).

It seems that a process like slab break off at intermediate depths concentrate the down dip tensional stress in the earthquake nest, The negative buoyancy of slab (Chappel & Tullis, 1977), the concentrated tensional stress due to tearing of slab and the active process of dehydration embrittelment (Hacker *et al.*, 2003) create right environment for occurrence of numerous earthquakes with thrust mechanism in the nest, like in the case of the Vrancea. In the case of collision between two subducted slab, it seems that both negative buoyancy and direction of collision are the controlling parameters in the mechanism of earthquakes. If collision be able to explain the nature of the Bucaramanga and the Hindu Kush nests, direction of collision may explain the differences in the observed mechanism of the earthquakes in these two nests. The seismicity in the case of Hindu Kush, indicates collision from opposite direction, while the Bucaramanga nest seems to be created due to frictional slip of two subducted slabs beside each other with different orientation. If existence of CLVDs at intermediate depths can be explained by source complexity, it seems that collision can perturb the stress field and produce the non-double couple earthquakes. This may be explained by the fact that the high percentage of CLVDs are present both in the Bucaramanga and the Hindu Kush nests and don't exist in the Vrancea nest (Based on Harvard Catalog).

Studying Makran subduction zone shows that collision zones in the east and the west of the Makran subduction zone can modify the state of stress in the overriding lithosphere and influence the stress field. Non-existence of large earthquakes does not necessarily indicate weak coupling in the slab interface. In fact, the observed highly negative TPGA and TPTA in the fore-arc setting of the western Makran can indicate high coefficient of friction and hence strong coupling, according to Song & Simons (2003), in the slab interface. The high coefficient of friction and the low velocity of convergence can slow down the process of shear stress build up and affect the seismogenic behavior in the fore-arc setting. According to Song & Simons (2003), the Kamchatka earthquake in 1952 is located in an area with both positive and negative TPGA and TPTA. Our investigation also show that both large earthquakes in the eastern Makran in 1851 and 1945 are located in the areas with positive TPGA and TPTA. Although, it has been shown that the total seismic moment release decreases by increasing the magnitude of TPGA almost world wide (Song & Simons, 2003), but in some areas like those mentioned above this observation cannot be justified. According to Pacheco *et al.* (1993), irregularities in the subducting slab such as subduction of a sea-mount can associate the slab interface to unstable frictional behavior. Unstable frictional behavior indicates strong coupling in the slab interface. Subduction of sea-mounts can produce high TPGA and TPTA in the fore-arc setting and should be considered as a likely mechanism for producing the 1851 and the 1945 earthquakes in Makran or the 1952 earthquake in Kamchatka.

Observations in the subduction zones with strong coupling in the slab interface show that the stress change within a cycle of earthquake and the intermediate depths normal faults can be a good indicator of the mature stages of an earthquake cycle (Malgrange *et al.*, 1981; Dziewonski & Woodhouse, 1983; Lovison, 1986; McNally *et al.*, 1986). A recent earthquake supporting this hypothesis, is the Nov. 2006 earthquake in Kuril, which has been predicted by Dmowska & Lovison (1988). In subduction zones with several known large earthquakes in the slab interface, like Makran, the measurement of rate and magnitude of deformation in the overriding lithosphere can help to understand which area of slab interface is closer to the future large earthquakes.

5. Conclusions

We summarize the result of our investigations in the area of unusually high and low level of seismicity in subduction zones as follow:

- Earthquake nests, which are not associated with volcanic activity, have a b-value of less than 1.73 suggesting no swarm activity in the nest. Their largest reported earthquake is of moderate magnitude (M_b=5.9-6.5), their moment release is higher than that of the surrounding areas and they mostly experience thrust faulting as the dominant mechanism inside the nest.

- Reviewing all earthquake nests not related to volcanic activity has revealed that the Bucaramanga nest is the smallest, the most active and the most disputed earthquake nest.

- The local seismicity in Colombia suggests that two slabs with two different dip angles ($25°$ in the north and $50°$ in the south) exist in the area of the Bucaramanga nest. The dip angle of the Bucaramanga nest ($29°$) is more in agreement with the northern slab.

- The focal mechanism stress inversion of moderate size earthquakes shows that the Bucaramanga nest is experiencing down dip tension where the plunge of σ_3 is in good agreement with the dip angle of the southern slab.

- The concentration of seismic activity in a small volume of the Bucaramanga nest, the variation in the mechanism of earthquakes and the complexity in the source of earthquakes inside the nest, can be explained by collision between the two subducting slabs in the area of the Bucaramanga nest. We used a 3D FE model to test this idea.

- The Makran subduction zone experiences two different states of stress in its overriding lithosphere. The overriding lithosphere stress field in the west is under the influence of collision between Arabia and Eurasia and in the east under the influence of collision between India and Eurasia.

- The Sistan suture zone, which is the boundary between the two segments (Lut and Helmand blocks) in the overriding lithosphere, may have a thick root. It is possible that the root of the suture zone meets the low dip angle slab at intermediate depths around 58 km and produces complexity in the source of earthquakes occurring in that depth.

- The high negative TPGA and TPTA (<-50 mGal and <-750 m) in the western Makran suggest strong coupling in that region. It means that the overriding lithosphere is dragged down by the subducting lithosphere due to a high coefficient of friction in the slab interface. We used a 2D elastic-viscoelastic FE model to show that shear stress build-up in the western Makran is a slow process and it may explain the lack of seismic activity in this region at the present time.

- The eastern and the western Makran, in the fore-arc setting, seem to be separated by an area with high positive TPGA and TPTA.

- The existence of normal faults at intermediate depths in the Makran subduction zone indicate the stages of a mature cycle of earthquake in mainly two segments. The segment of the western Makran and the segment associated with the 1851 earthquake rupture zone.

- We used a 2D elastic-viscoelastic FE model to estimate the deformation in the overriding lithosphere above the slab interface with heterogeneous coupling for different cycle of earthquakes. The result shows that deformation is more pronounced above the strongly coupled part of the slab interface.

- Our 2D FE modelling shows that the shorter the length of the cycle, the faster is the rate of deformation. As a result we expect faster rate of deformation in the eastern Makran compared to the western Makran.
- Considering the fact that in the middle of a cycle the induced extensional stress at intermediate depth is insignificant and cannot explain the observed normal faults in Makran, we constrain the recurrence time of earthquakes with the size of the 1851 event to shorter than 300 years.
- The overriding lithosphere in the beginning of the cycle experiences uplift and towards the end of the cycle experiences subsidence. Assuming that the 1945 and the 1851 earthquakes in the eastern Makran have almost the same magnitude, we believe that at the present time, the overriding lithosphere above the 1851 earthquake should experience considerable subsidence, while the overriding lithosphere above the 1945 earthquake experiences uplift.

6. Future work in the areas addressed in this thesis

We consider our work as a starting step towards understanding the nature of unusual seismicity in subduction zones. We believe we can achieve better results in the future if we consider the following:

- Among the possible earthquake nests, Fiji nest looks unique. It is not clear why earthquakes with thrust mechanism should be observed at that depth (570-620 km). This area should be investigated from the seismological and tectonophysical point of view in more detail.
- Since the two slabs around the Bucaramanga nest have two different age and evolution time, it seems appropriate that a more advanced 3D thermo-mechanical model which also involve the thermal structure of the slabs be developed. The difference in the thermal structure of slabs may give rise to differences in the rate or concentration of seismic activity in the collision zone.
- In order to understand any interaction between the Sistan suture zone and the subducted slab in Makran, a regional tomography investigation is necessary.
- In order to address the deformation within an earthquake cycle in the overriding lithosphere in Makran more accurately and by using a 3D FE model, continuous and dense geodetic observation in the future will be necessary.

References

Adams, J. (1990). Paleoseismicity of the Cascadia subduction zone: Evidence from turbidites off the Oregon-Washington margin. *Tectonics,* **9**, 569–583.

Aki, K. (1979). Characterization of barriers on an earthquake fault. *J. Geophys. Res.* **84**, 6140–6148.

Ambraseys, N. & Melville, C. (1982). *A History of Persian Earthquakes*. Cambridge University Press, New York.

Ansys-ED (2005). *Ansys Theory Reference*. Ansys Co.,London, UK.

Atwater, B. (1995). Consensus about past great earthquakes at the Cascadia subduction zone. *Earthquake Spectra,* **11**, 1–18.

Becker, T. (2002). Lithosphere-Mantle intercations. *Ph.D. thesis, Harvard University,* .

Billington, S., Isacks, B. L. & Barazangi, M. (1977). Spatial distribution and focal mechanisms of mantle earthquakes in the Hindu Kush-Pamir region: A contorted Benioff zone. *Geology,* **5**, 699–704.

Bird, P. (2003). An updated digital model of plate boundaries. *Geochemistry, Geophysics, Geosystems,* **4(3)1027**, doi:10.1029/2001GC000252.

Bleahu, M. D., Boccaletti, M., Manetti, P. & Peltz, S. (1973). Neogene Carpathian Arc: a continental arc displaying the features of an 'island arc'. *J. Geophys. Res.* **78**, 5025–5032.

Blot, C. (1981*a*). Earthquakes at depth beneath volcanoes, forerunners of their activities, application to White Island, New Zealand. *J. Volcanol. Geotherm. Res.* **9**, 277–291.

Blot, C. (1981*b*). Deep root of andesitic volcanoes: new evidence of magma generation at depth in the Benioff zone,. *J. Volcanol. Geotherm. Res.* **10**, 339–364.

Burtman, V. S. & Molnar, P. (1993). Geological and Geophysical evidence for deep subduction of continental crust beneath the Pamir. *Geol. Soc. of Am., Spec. Pap.,* **281**.

Byrne, D. E., Sykes, L. & Davis, D. M. (1992). Great thrust earthquakes and aseismic slip along the plate boundary of the Makran subduction zone. *J. Geophys. Res.* **97**, 449–478.

Carayannis, G. P. (2006). The potential of tsunami generation along the Makran subduction zone in the northern Arabian sea. case study: the earthquake and tsunami of November 28, 1945. *Science of Tsunami Hazard,* **24**, 358–384.

Carr, M. J. (1983). Nests of intermediate depth (70-160 km) earthquakes adjucent to active volcanoes during 1963-1982. *J. Volcanol. Geotherm. Res.* **19**, 349–365.

Carr, M. J. & Stoiber, R. E. (1973). Intermediate depth earthquakes and volcanic eruptions of Fuego volcanoes in Guatemala. *EOS,* **57**, 346.

Chappel, W. M. & Tullis, T. E. (1977). Evolution of the forces that drive the plates. *J. Geophys. Res.* , 1967–1984.

Chatelain, J. L., Roecker, S. W., Hatzfeld, D. & Molnar, P. (1980). Microearthquake seismicity and fault plane solutions in Hindu Kush region and their tectonic implications. *J. Geophys. Res.* **85**, 1365–1387.

Chen, P. F., Bina, C. R. & Okal, E. A. (2001). Variations in slab dip along the subducting Nazca plate, as related to stresss patterns and moment release of intermediate-depth seismicity and to the surface volcanism. *Geochemistry, Geophysics, Geosystems,* **2**, 2001GC000153.

Cortes, M. & Angelier, J. (2005). Current states of stress in the northern Andes as indicated by focal mechanisms of earthquakes. *Tectonophysics,* **403**, 29–58.

De Mets, C., Gordon, R. G., Argus, D. F. & Stein, S. (1990). Current plate motions. *Geophys. J. Int.* **101**, 425–478.

Dewey, J. & Bird, J. (1970). Mountain belts and the new global tectonics. *J. Geophys. Res.* **75**, 2625–2647.

Dewey, J. F. (1972). Seismicity and tectonics of western Venezuela. *Bull. Seismol. Soc. Am.* **62**, 1711–1752.

Dmowska, R. & Lovison, L. (1988). Intermediate-term seismic precursors for some coupled subduction zones. *Pure Appl. Geophys.* **126**, 643–664.

Dmowska, R., Rice, J. R., Lovision, L. C. & Josell, D. (1988). Stress transfer and seismic phenomena in coupled subduction zones during the earthquake cycle. *J. Geophys. Res.* **93**, 7869–7884.

Dziewonski, A. M., Friedman, A., Giardini, D. & Woodhouse, J. H. (1983). global seismicity of 1982: Centroid- moment tensor solution for 308 earthquakes. *Phys. Earth Planet. In.* **33**, 76–90.

Dziewonski, A. M. & Woodhouse, J. H. (1983). An experiment in systematic study of global seismicity: Centroid-moment tensor solution for 201 moderate and large earthquakes of 1981. *J. Geophys. Res.* **88**, 3247–3271.

Engdahl, E. R. (1977). Seismicity and plate subduction in the central Aleutians. In *Island arcs, Deep Sea Trenches and Back Arc Basins* pp. 259–271. Am. Geophys. Union, Washington, D.C.

Engdahl, E. R. & Villasenor, A. (2002). Global seismicity: 1900-1999. In *International Handbook of Earthquakes and Engineering Seismology*. Elsevier Science Ltd.

Fan, G., Ni, J. F. & Wallace, T. C. (1994). Active tectonics of the Pamirs and Karakorum. *J. Geophys. Res.* **99**, 7131–7160.

Farhoudi, G. & Karig, D. E. (1977). Makran of Iran and Pakistan as an active arc system. *Geology,* **5**, 664–668.

Fitch, T. J. & Scholz, C. H. (1971). Mechanism of underthrusting in southwest Japan: A model of convergent plate interaction. *J. Geophys. Res.* **76**, 7260–7292.

Fluck, P., Hyndman, R. D. & Wang, K. (1997). Three dimensional dislocation model for great earthquakes of the Cascadia subduction zone. *J. Geophys. Res.* **102**, 20539–20550.

Forsyth, D. & Uyeda, S. (1975). On the relative importance of the driving forces of plate motion. *Geophys. J. R. Astr. Soc.* **43**, 103–162.

Freymueller, J. T., Kellogg, J. N. & Vega, V. (1993). Plate motions in the North Andean region. *J. Geophys. Res.* **98**, 21853–21863.

Frohlich, C., Kadinsky-cade, K. & Davis, S. D. (1995). A re-examination of the Bucaramanga Colombia, earthquake nest. *Bull. Seismol. Soc. Am.* **85**, 1622–1634.

Frohlich, C., Riedesel, M. A. & Apperson, K. D. (1989). Note concerning possible mechanisms for non-double-couple earthquake sources. *Geophys. Res. Lett.* **16**, 523–526.

Hacker, B., Peacock, S., Abers, G. & Holloway, S. (2003). Subduction factory 2. Are intermediate-depth earthquakes in subducting slabs linked to metamorphic dehydration reactions? *J. Geophys. Res.* **108**, doi:10.1029/2001JB001129.

Hackney, R., Gotze, H. J. & Meyer, U. (2005). Topographic, bathymetric and gravity characteristics of convergent margins. *Geotechnologien Science Report,* **5**, 30–33.

Hassani, R., Jongmans, D. & Chery, J. (1997). Study of plate deformation and stress in subduction processes using two dimensional numerical models. *J. Geophys. Res.* **102**, 17951–17965.

Hyndman, R. D. & Wang, K. (1995). The rupture zone of Cascadia great earthquakes from current deformation and thermal regime. *J. Geophys. Res.* **154**, 10022–13322.

Isacks, B. L., Sykes, L. R. & Oliver, J. (1967). Spatial and temporal clustering of deep and shallow earthquakes in the Fiji- Tonga- Kermadec region. *Bull. Seismol. Soc. Am.* **57**, 935–958.

Kearey, P. & Vine, F. J. (1996). *Global Tectonics*. Second edition, Blackwell Science Ltd, MA 021485018, USA.

Kellogg, J. H. & Vega, V. (1995). Tectonic development of Panama, Costa Rica and the Colombian Andes: Constraints from Global Positioning System, geodetic studies and gravity. *Spec. Pap. Geol. Soc. Am.* **295**, 75–90.

Kikuchi, M. & Kanamori (2003). *Note on teleseismic Body-wave inversion program.* www.eri.u-tokyo.ac.jp/ETAL/KIKUCHI.

Kirby, S., Engdahl, E. & Denlinger, R. (1996). *Intermediate-depth intraslab earthquakes and arc volcanism as physical expressions of crustal and uppermost mantle metamorphism in subducting slabs.* Subduction: Top to Bottom, Geophys. Monogr. Ser., Vol. 96.

Lin, S. & Van Keken, P. (2005). Dynamics of thermomechanical plumes:2. complexity of plume structure and its implications for mapping mantle plumes.

Lithgow-Bertelloni, C. & Richards, M. (1995). Cenozoic plate driving forces. *Geophys. Res. Lett.* **22**, 1317–1320.

Lovison, L. C. (1986). Seismicity variation throughout the Middle American Trench subduction earthquake cycle. Master's thesis Harvard University, Cambridge, Mass.

Lukk, A. A. & Nersesov, J. L. (1965). Structure of the upper part of the Earth's mantle from the observations of intermediate depth earthquakes. In *Proc. (Dokl.) Acad. Sci. USSR,(in Russian)* pp. 559–562, Acad. Sci. USSR.

Lukk, A. A. & Vinnik, L. P. (1975). Tectonic interpretation of the depth structure of the Pamirs. *Geotectonics,* **5**, 73–80.

Maggi, A., Jackson, J. A., Priestley, K. & Baker, C. (2000). A re-assessment of focal depth distribution in southern-Iran, the Tien Shan and northern India: Do earthquakes really occur in the continental mantle? *Geophys. J. Int.* **143**, 629–661.

Malave, G. & Suarez, G. (1995). Intermediate- depth seismicity in northen Colombia and western Venezuela and its relationship to Caribbean plate subduction. *Tectonics,* **14**, 617–628.

Malgrange, M., Deschamps, A. & Madariaga, R. (1981). Thrust and extensional faulting under the Chilean coast:1965, 1971 Aconcagua earthquakes. *Geophys. J. R. Astron. Soc.,* **66**, 313–331.

Marotta, A. M. & Mongelli, F. (1998). Flexure of subducted slabs. *Geophys. J. Int.* **132**, 701–711.

McNally, K. C., Gonzalez-Ruiz, J. R. & Stolte, C. (1986). Seismogenesis of the 1985 great (Mw=8.1) Michoacan, Mexico earthquake. *Geophys. Res. Lett.* **13**, 585–588.

McNutt, M. K. & Menard, H. W. (1982). Constraints on yield strength in the oceanic lithosphere derived from observations of flexure. *Geophys. J. R. Astron. Soc.,* **71**, 363–394.

Michael, A. (1984). Determination of stress from slip data: Faults and folds. *J. Geophys. Res.* **89**, 11517–11526.

Michael, A. (1987*a*). Stress rotation during the Coalinga aftershocks sequence. *J. Geophys. Res.* **92**, 7963–7979.

Michael, A. (1987*b*). Use of focal mechanisms to determine stress: A control study. *J. Geophys. Res.* **92**, 357–368.

Michael, A. (1991). Spatial variation of stress within the 1987 Whittier Narrow, California, aftershock sequence: new techniques and results. *J. Geophys. Res.* **96**, 6303–6319.

Montagner, J. & Kennet, B. (1995). How to reconcile bodey-wave and normal mode reference earth models. *Geophys. J. Int.* **125**, 229–248.

Nilforoushan, F., Masson, F., Vigny, C., Martinod, J., Nankali, H., Hatzfeld, D., Bayer, R., Tavakoli, F., Ashtiani, A., Doerflinger, E., Daignieres, M., Collard, P. & Chery, J. (2003). GPS network monitors the Arabia-Eurasia collision deformation in Iran. *Journal of Geodesy,* **77**, 411–422.

Nowroosi, A. A. (1972). Focal mechanism of earthquakes and plate tectonics of Middle east. *Bull. Seismol. Soc. Am.* **62**, 823–850.

Nowroozi, A. A. (1971). Seismo-tectonics of the Persian Plateau, Eastern Turkey, Caucasus, and Hindu Kush regions. *Bull. Seismol. Soc. Am.* **61**, 317–341.

Ojeda, A. & Havskov, J. (2001). Crustal structure and local seismicity in Colombia. *J. Seismol.* **5**, 575–593.

Oncescu, M. C. (1984). Deep structure of Vrancea region, Romania, inferred from simultaneous inversion for hypocenters and 3-D velocity structure. *Ann. Geophys.,* **2**, 23–28.

Oncescu, M. C. (1986). Relative seismic moment tensor determination for Vrancea intermediate depth earthquakes. *Pure Appl. Geophys.* **124**, 931–940.

Oncescu, M. C. (1987). On the stress tensor in Vrancea region. *J. Geophysics,* **62**, 62–65.

Pacheco, J. F., Syskes, L. R. & Scholz, C. H. (1993). Nature of seismic coupling along simple plate boundaries of the subduction type. *J. Geophys. Res.* **98**, 14133–14159.

Page, w. D., Alt, J. N., Cluff, L. S. & Plafker, G. (1979). Evidence for recurrence of large-magnitude earthquakes along the Makran coast of Iran and Pakistan. *Tectonophysics,* **52**, 533–547.

Pennington, W. D. (1981). Subduction of the eastern Panama basin and seismotectonics of north western South America. *J. Geophys. Res.* **86**, 10753–10770.

Quittmeyer, R. C. & Jacob, K. H. (1979). Historical and modern seismicity of Pakistan, Afghanistan, northwestern India, and southeastern Iran. *Bull. Seismol. Soc. Am.* **69**, 773–823.

Quittmeyer, R. C. & Kafka, A. L. (1984). Constraints on plate motions in southern Pakistan and northern Arabian Sea from the focal mechanism of small earthquakes. *J. Geophys. Res.* **89**, 2444–2458.

Richardson, E. & Jordan, T. (2002). Low frequency properties of intermediate focus earthquakes. *Bull. Seismol. Soc. Am.* **92**, 2434–2448.

Ruff, L. J. (1989). Do trench sediments affect great earthquake occurrence in subduction zone? *Pure Appl. Geophys.* , 263–282.

Sacks, I. S., Suyehiro, S., Kamitsuki, A., Tuve, M. A., Otsuka, M., Saa, G., Rodriguez, A., Gajardo, E., Cabre, R., Fernandez, L., Valponi, F., Giesecke, A. & Aldrich, L. T. (1966). A tentative value of Poisson's coefficient from the seismic "nest of Socompa, Annual report of the Director, Carnegie Inst.". Technical report Dep. of Terr. Magn.

Santo, T. (1969). Regional study on the characteristic seismicity of the world, I, Hindu kush region. *Bull. Earthquake Res. Inst., Tokyo Univ.,* **47**, 1035–1049.

Satake, K., Shimazaki, K., Yoshinobu, T. & Ueda, K. (1996). Time and size of the giant earthquake in Cascadia inferred from Japanese tsunami records of january 1700. *Nature,* **379**, 246–249.

Schneider, J. F., Pennington, W. & Meyer, R. P. (1987). Microseismicity and focal mechanisms of the intermediate depth Bucaramanga nest, Colombia. *J. Geophys. Res.* **92**, 13913–13926.

Shemenda, A. I. (1994). *Subduction:Insights from Physical Modeling*. Kluwer Academic Publisher, London, U.K.

Shih, X. R., Meyer, R. P. & Schneider, J. F. (1991*a*). Seismic anisotropy above a subducted plate. *Geology,* **19**, 807–810.

Shih, X. R., Schneider, J. F. & Meyer, R. P. (1991*b*). Polarities of P and S waves, and shear wave splitting observed from the Bucaramanga nest, Colombia. *J. Geophys. Res.* **96**, 12069–12082.

Song, T. A. & Simons, M. (2003). Large trench parallel gravity variation perdict seismogenic behavior in subduction zones. *Science,* **301**, 630–633.

Sperner, B., Lorenz, F., Bonjer, K., Hettel, S., Muller, B. & Wenzel, F. (2001). Slab break off-abrupt cut or gradual detachment? New insights from Vrancea region (SE Carpathians, Romania). *Terra Nova,* **13**, 172–179.

Stein, S., Engeln, J. F., Wiens, D. A., Fujita, K. & Speed, R. C. (1982). Subduction seismicity and tectonics in the Lesser Antilles arc. *J. Geophys. Res.* **87**, 8642–8664.

Taboada, A., Rivera, L. A., Fuenzalida, A., Cisternas, A., Philip, H., Bijwaard, H., Olaya, J. & Rivera, C. (2000). Geodynamics of the northern Andes: Subduction and intercontinental deformation (Colombia). *Tectonics,* **19**, 787–813.

Taylor, M. A. J., Zheng, G., Rice, J. R., Stuart, W. D. & Dmowska, R. (1996). Cyclic stressing and seismicity at strongly coupled subduction zone. *J. Geophys. Res.* , 8363–8381.

Tirrul, R., Bell, I. R., Griffis, R. J. & Camp, V. E. (1983). The Sistan suture zone of eastern Iran. *Geol. Soc. Am. Bull.* **94**, 134–150.

Tryggvason, E. & Lawson, JR, E. (1970). The intermediate earthquake source near Bucaramanga, colombia. *Bull. Seismol. Soc. Am.* **60**, 269–276.

Turcotte, D. L. & Schubert, G. (2002). *Geodynamics*. Second edition, Cambridge University Press, Cambridge.

Usami, T. & Watanabe, T. (1980). Definition and characteristic features of seismically active region (earthquake nest) in Kanto dirstrict. *Pure Appl. Geophys.* **118**, 1326–1328.

Van der Hilst, R. & Mann, P. (1994). Tectonic implication of tomographic images of subducted lithosphere beneath northwestern South America. *Geology,* **22**, 451–454.

Wells, R. E., Blakely, R. J., Sugiyama, Y., Scholl, D. W. & Dinterman, P. (2003). Basin centered asperities in great subduction zone earthquakes: A link between slip, subsidence and subduction erosion. *J. Geophys. Res.* **108**, doi:10.1029/2002JB002072.

Zheng, G., Dmowska, R. & Rice, J. R. (1996). Modeling earthquake cycles in the Shumagin subduction segment, Alaska, with seismic and geodetic constrains. *J. Geophys. Res.* **101**, 8383–8392.

Part II.

Papers